ISSS Journal of Micro and Smart Systems (2020) 9:1–32
https://doi.org/10.1007/s41683-020-00050-5

REVIEW PAPER

# A half a decade timeline of shape memory alloys in modeling and applications

S. Kumar[1] · P. Shivashankar[1] · S. Gopalakrishnan[1]

Received: 17 January 2020 / Revised: 10 March 2020 / Accepted: 13 March 2020 / Published online: 20 March 2020


**Abstract**
To unlock the lock of futuristic developments, nowadays shape memory alloys (SMAs) are acting as key by outnumbering the existing smart materials in view of new design competence, innovative techniques, enhanced technologies, and meeting the dire need according to the demand of ongoing scientific and industrial progress. Undoubtedly, it can be worthy to associate SMAs with the term polymorphism, as they possess unique capability to encapsulate multitudinous inherent characteristics under their name. Shape memory effect, superelasticity, and damping are there to name a few among many others, as prime indicators. The exhibition of these characteristics of SMAs is due to the transformation that takes place between austenite phase and martensite phase which is achieved either by temperature or stress variation. The fascinating characteristics they possess enable them to attract researchers and designers toward their potential applications in diverse domain as smart and multi-functional materials. The present work focuses on the review of research works accomplished in the recent 5 years pertaining to modeling and applications of shape memory alloys in distinct domains. Under the topic of modeling, a look into the research carried out on a variety of SMA structures—like functionally graded SMAs, SMA springs, porous SMAs, novel SMA actuators—is presented. In addition to this, the work carried out to represent SMAs with large strains and large rotations and to model polycrystalline SMAs is also covered. This is supplemented by application-oriented domains, each of which disseminates the attributes of SMAs that are self-sufficient to express what factors make SMAs more prominent. It is believed that the foregoing works comprehensively detailed in this review article will certainly lay a solid platform for the future investigations that are going to take place in time to come.

**Keywords** Shape memory alloy · Shape memory effect · Superelasticity · Constitutive model · Porous SMA · SMA spring · Functionally graded SMA · Polycrystalline SMA · SMA actuator · Construction · Biomedical · Aerospace · Offshore

## Introduction

With the passage of time, the amalgamation of materials with distinct material properties has led to the development of novel alloys that can potentially be utilized in a wide spectrum of applications. This has been made possible because of the necessity of the present time to have lighter and durable materials, with tailored properties, which can make them available as and when needed, to perform multi-functional operations. It is due to this amalgamation process, past decades have witnessed the development of shape memory alloys.

Since their recognition in early 1960s, shape memory alloys have made and are still making, their presence felt in this cutting-edge scientific and technological era by being in the forefront among all the smart materials. Owing to their unique and inherent characteristics, SMAs have drawn significant attention and perpetual interest of the concerned leaders toward both general scientific research and specific commercial applications. The innovative notions, practical applications, and manufacturing of

✉ S. Kumar
santankumar@iisc.ac.in

✉ P. Shivashankar
shivashankar@iisc.ac.in

✉ S. Gopalakrishnan
krishnan@iisc.ac.in

[1] Department of Aerospace Engineering, Indian Institute of Science, Bangalore 560012, India

desirable goods (pertaining to the SMAs) have offered room for development of novel distinct SMAs that can be utilized from micro-level to macro-level. In view of this, several attempts across the globe have been taken into account to brush up and avail their existing properties in order to enlarge their application driven potentials.

This work aims to impart a brief and informative aspects of shape memory alloys and their associated phenomenon, modeling philosophy of SMA along with a detailed elaboration on SMA applications. To be specific, SMA applications form different segregate subsections depending upon the domain of applications viz. construction, biomedical, aerospace, and offshore. An in-depth review and recent progress in these aforementioned applicative sectors are profoundly compiled to present them in a lucid manner. Finally, the highlights of the current state of the art in the form of concluding remarks have been listed out, which is followed by discussion on future research possibilities. These pointed out facts may act as torch bearer by paving way for the development of novel SMAs, and thereby, opening doors for new modeling and applications opportunities in years to come.

## Shape memory alloys and their associated phenomenon

Being one of the smart materials and belonging to the class of shape memory materials (SMMs), SMAs, among all SMMs, have been able to catch the eyeballs of the smart material community and are, therefore, now, a well-explored domain. Shape memory alloys are a group of metallic alloys which display shape memory behavior together with their additional inherent characteristics—be they physical, thermal, mechanical, or electrical. These alloys possess excellent capability to restore their pre-deformed shape and size when heated above their transition temperatures after undergoing deformation in their lower temperature phase. This impeccable strain recovery behavior displayed by SMAs has unarguably brought them in industrial and technological arena where strain recovery is of paramount importance.

As shape memory alloys are capable of recovering their original shape, due to phase transformations they undergo, by means of temperature and stress fields, these alloys are primarily characterized by three unique thermomechanical behaviors: firstly, shape memory effect (SME) which may be one-way SME or two-way SME; secondly, pseudoelastic effect also known as superelasticity and thirdly, damping. As a matter of fact, the temperature-induced transformation forms the basis of one-way and two-way shape memory effect, while pseudoelastic effect follows the stress-induced transformation. This is illustrated in Fig. 1.

In an absolutely precise way, the shape memory effect refers to the ability of retaining the deformed shape up to heat induced retrieval of the original shape, whereas the pseudoelastic effect refers to the potential of restoring the original shape after large nonlinear deformations which are induced by mechanical load in the absence of heating. In particular, one-way SME involves maintaining a deformed state even after the external force is removed (which on heating returns back to its original shape). On the other hand, two-way SME, or reversible SME, describes the

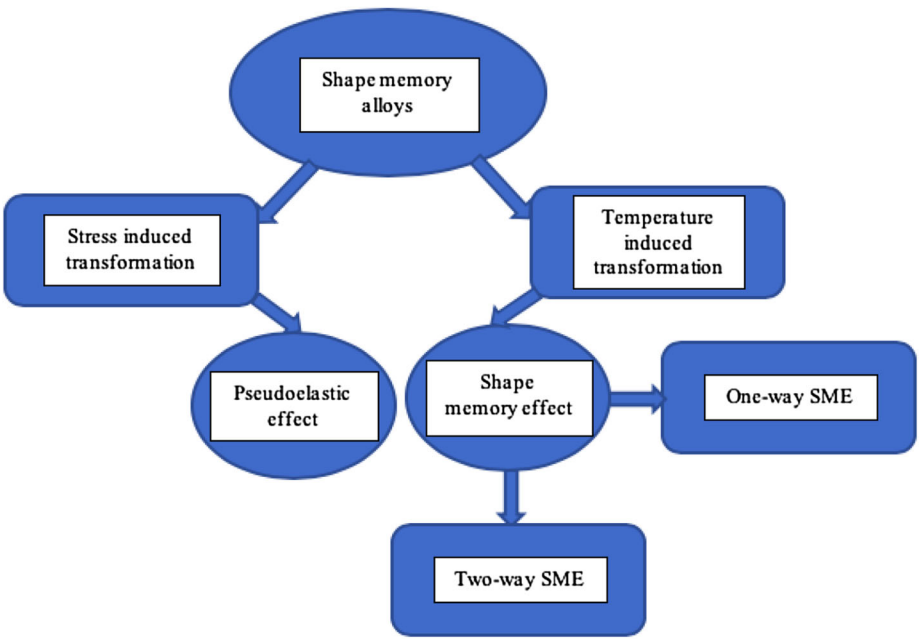


**Fig. 1** Classification of shape memory alloys

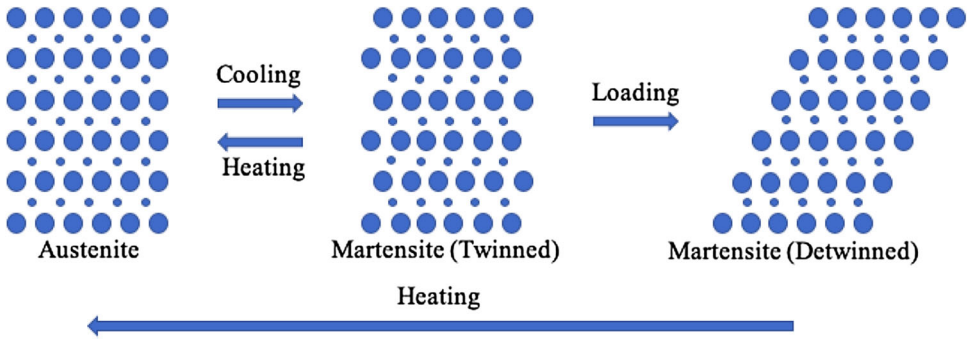


**Fig. 2** Phase transformation of shape memory alloys, adapted from Ghassemieh et al. (2017)

ability of SMA to remember two distinct shapes—one at low and one at high temperature. Damping corresponds to the capability of transforming mechanical energy into thermal energy. These aforementioned unique characteristics of SMAs are consequence of thermoelastic martensitic transformation.

Shape memory alloys usually exist in two crystalline phases viz. austenite phase and martensite phase. The occurrence of solid-solid phase transformation is non-diffusive, and hence is called martensitic. The solid phase achieved upon cooling is called martensite. Austenite is called the parent phase in which transformation process occurs. The austenite phase is considered to be stable at high temperature, while the martensite phase is often found to be stable at low temperature. Both these phases differ in their crystal structures. Austenite holds high symmetry cubic structure and is, therefore, found in strong phase. Martensite, on the other hand, bears an asymmetric parallelogram structure and is, therefore, observed in weak phase (and hence can be readily deformed). The transformation of SMA from austenite phase to martensite phase may be acquired either by temperature or stress variation. When achieved through temperature variation, it results in twinned or multi-variant martensite, and when induced through stress variation, it leads to detwinned or single-variant martensite. The phase transformation of shape memory alloys is delineated in Fig. 2.

A detailed overview of shape memory alloys and their applications along with design aspects is well documented in a number of monographs (Otsuka and Wayman 1999; Lagoudas 2008; Yoneyama and Miyazaki 2008; Miyazaki et al. 2009; Yamauchi et al. 2011; Duerig et al. 2013; Rao et al. 2015). Moreover, to bridge the gap between the past development and the recent progress of SMAs, this article covers a good amount of review works (Miyazaki and Otsuka 1989; Van Humbeeck et al. 1991; Otsuka and Ren 1999; Wu and Lin 2000; Van Humbeeck 2001; Cai et al. 2005; Hassan et al. 2013; Jani et al. 2014; Lobo et al. 2015; Naresh et al. 2016; Peng et al. 2018) that have been published over the years. These review articles highlight all the research and applications so far. In addition to the above mentioned phenomenon associated with SMAs, they face certain challenges, such as (1) durability and reliability, (2) low energy efficiency, (3) high manufacturing cost, (4) low operational frequency and narrow bandwidth, and (5) overheating, overstressing, and overstraining. These challenges can be dealt by means of suitable measures, for instance (1) thermomechanical treatment, (2) number of transformation cycles, (3) advancement in development and processing of materials, (4) appropriate loading conditions, (5) mechanical design optimization, (6) changing the shape and size of SMA, and (7) using SMA where energy efficiency is not of much importance. The transformation properties, mechanical properties, physical properties and other relevant aspects of commonly used NiTi SMA are outlined in Table 1.

## Analytical and numerical models on various SMA structures

In this section, the recent work carried out in developing models for various SMA structures is presented. As such, this section focuses on covering studies that have developed models for new SMA structures, new concepts with SMAs, and novel SMA actuators. In this context, it tries to follow the footsteps of several review articles (Birman 1997; Matsuzaki and Naito 2004; Paiva and Savi 2006; Khandelwal and Buravalla 2009; Cisse et al. 2016a), and picks up the research activities that has been conducted since the publication of last review (Cisse et al. 2016a). It must also be noted that the section does not cover research conducted on the "secondary effects" of the SMA (Cisse et al. 2016b), as this falls out of the scope of the article.

### Functionally graded SMA and FGM/SMA structure

Due to the development of a few production methods of FG-SMA in the last decade, and due to the relatively superior mechanical properties of FG-SMA—such as the liberty offered in choosing the type of material for different parts, the continual distribution of material components,

**Table 1** Characteristics of NiTi shape memory alloy, adapted from Weirich and Kuhlenkötter (2019)

| Properties-based classification | NiTi characteristics | NiTi specifics |
|---|---|---|
| Transformation properties | Temperature hysteresis | $\sim 30\,(\mathrm{K})$ |
| | Transformation temperature | $-100$ to $+100\,(^{\circ}\mathrm{C})$ |
| | Specific energy density | 3000 (J/kg) |
| | Maximum attainable strain (one-way effect) | 8 (%) |
| | Maximum attainable strain (two-way effect) | 4–6 (%) |
| | Maximum attainable strain (pseudoelastic effect) | 7 (%) |
| | Typical number of cycles | 100,000 |
| Mechanical properties | Admissible stress for actuator cycling | 50–150 (MPa) |
| | Young's modulus | 35–70 (GPa) |
| | Yield strength | 70–690 (MPa) |
| | Tensile strength | 800–1000 (MPa) |
| | Elongation to failure | 40–50 (%) |
| Physical properties | Density | 6.45 ($\mathrm{g/cm^3}$) |
| | Thermal conductivity | 6.6–10 ($10^{-6}\,\mathrm{K^{-4}}$) |
| | Electrical resistivity | 0.5–1.1 ($10^{-6}\,\Omega\mathrm{m}$) |
| | Corrosion resistance | Very good |
| | Biological compatibility | Very good |
| Others | Processing | Difficult |
| | Price | Expensive |
| | Sensor function | Intrinsic |

anti-friction properties, and hardness—mechanical couplers made of FG-SMA are preferred over those of dense SMA. The consequence of using FG-SMA, however, is the variation of behavior of the FG-SMA component with the gradient parameter. For an effective design of the component, this variation must be analyzed prior to the design.

One such study is the article by Liu et al. (2017), where a theoretical analysis for a FG-SMA cylinder, subjected to an internal pressure, was presented by the authors. Figure 3a shows the schematic diagram of the cylinder considered in the study. As a specific case, in the study, the critical phase transformation stresses and the maximum transformation strain were assumed to be non-gradient, while the Young's modulus ($E$) and the Poisson's ratio ($v$) were varied by an exponential function through its thickness (Eqs. 1, 2). $\beta$, the material parameter, which represents the functionally graded properties, can be either negative or positive. $E_0$ in the equation is given as $E_0 = (1-\xi)E_\mathrm{A} + \xi E_\mathrm{M}$, where $E_\mathrm{A}$ and $E_\mathrm{M}$ denote the Young's modulus in austenite and martensite states, with $\xi$ denoting the volume fraction of martensite.

$$E(r) = E_0 \exp\left(\frac{\beta(r-a)}{b-a}\right) \tag{1}$$

$$v(r) = v_0 \exp\left(\frac{\beta}{4}\frac{(r-a)}{b-a}\right). \tag{2}$$

Adopting an ideal elasto-plastic constitutive model, to simulate the phase transformation of the SMA, the analytical solutions were obtained. With this, for the thin

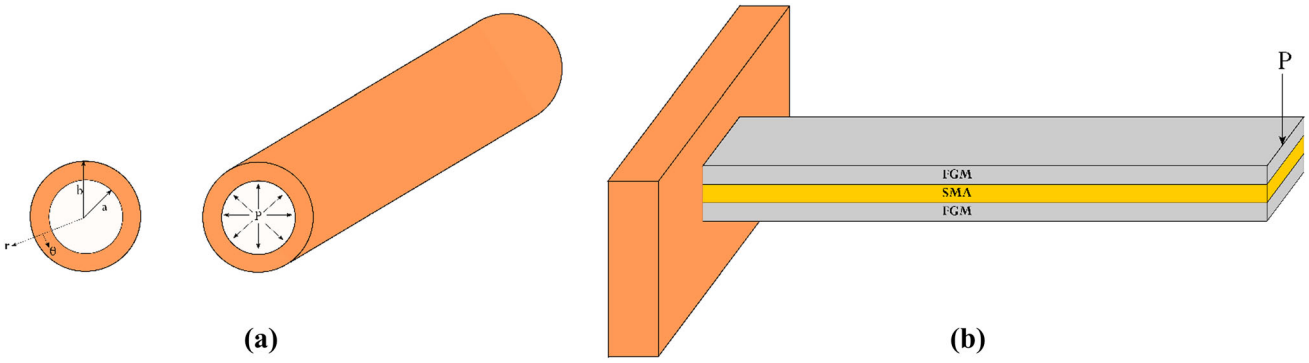


**Fig. 3** Schematic diagrams of **a** a SMA cylinder, adapted from Liu et al. (2017), **b** a cantilever FGM/SMA beam, adapted from Viet et al. (2018)

($a = 0.035$ m and $b = 0.040$ m) and thick ($a = 0.025$ m and $b = 0.040$ m) walled cylinder, the stress, strain, and displacement distributions were computed and plotted for different gradient parameters ($\beta = -2, -1, 0, 1, 2$). From the through-the-thickness plots, for the thin walled case, it was found that the normalized stress $-\sigma_r/p_a$ increased with the increasing $\beta$, with the curve for $\beta = 0$, being a straight line and those of $\beta = 1, 2$ being convex, and $\beta = -1, -2$ being concave. A plot of $\sigma_\theta/p_a$ showed that the normalized stress monotonically decreased with the radius for $\beta = -2, -1, 0$, and monotonically increased for $\beta = 1, 2$. Similar patterns were also found for most cases in the thick walled cylinder. This study showcased not only the modeling of a FG-SMA structure, but also the necessity of such analysis for the design of FG-SMA components.

Contrastingly, a cantilever FGM/SMA laminated composite beam was modeled by Viet et al. (2018). In their study, a SMA core is sandwiched between two FGM identical layers (as depicted in Fig. 3b), and a concentrated load is applied at the tip of the beam. The material properties in the FGM layers varied continuously across the thickness, and these properties were represented with power law functions. In case of the SMA, the constitutive equations derived based on the Zaki–Moumni model, developed in a previous study (Zaki and Moumni 2007), were used for modeling. Along with these constitutive equations, Timoshenko beam theory was used to account for the phase evolution during the loading and unloading cycle, and subsequently for modeling the dynamics of the beam. The closeness of the analytical curves, with the results from a numerical solution method and a 3D finite element analysis, validated the analytical model. Additionally, the effect on the superelasticity of a CNT-epoxy-based-FGM/SMA beam, due to several parameters (such as the gradient direction, gradient index, temperature, and relative thickness ratio) was studied.

## SMA springs

Heidari et al. (2016) fabricated SMA springs from two types of NiTi wires, through a process called the shape-setting process. In the shape setting treatment, a series of steps—which involve deforming, constraining, and applying heat treatment—are followed to transform the SMA into the desired shape. The core of their work was the investigation of the influence of the shape setting process on the thermomechanical properties (like the transformation temperatures, stiffness, and critical stress for transformation start) of the SMA springs. To state explicitly, in the fabricated springs, the behavior of the transformation temperature, the stiffness, and the intermediate phase (R-phase), start and finish temperature were investigated for changes in pitches and annealing temperatures. As far as the transformation temperatures were concerned, the pitch of the springs did not have a significant effect, but increase in the annealing temperature led to an increase in the transformation temperatures. The R-phase, start and finish temperatures, however, decreased with an increase in annealing temperature (with the R-phase disappearing at an annealing temperature of 600 °C). In the case of mechanical behavior, the pitch of the springs did have a significant effect. The Young's modulus also increased with the increasing annealing temperature. Further, an enhanced model, based on the Brinson's one-dimensional constitutive model with von-Mises yield criterion, was derived to study the shape memory effect, and the pseudoelasticity, in the springs. The numerical results from the model were validated with experimentation. Later, Zaki and Viet (2018) developed an analytical model for superelastic helical springs based on the Zaki–Moumni constitutive model. This model was developed for springs that had an index greater than 4, and pitch angle greater than 15° [the common configuration in practical engineering applications (Ancker 1958)].

In an attempt to model a SMA spring actuator, Cortez-Vega et al. (2018) developed a hybrid model—which provided an alternative for the characterization of the hysteresis in the SMA. The modeling is split into different stages, the first deals with the temperature variation of the actuator (in accordance with the supplied current). The following equation, based on the Joule effect, is used to describe the behavior of the temperature ($T$)–current ($i$) relationship

$$\frac{\mathrm{d}T(t)}{\mathrm{d}t} = \frac{i^2(t)R}{WC_\mathrm{w}} - \frac{hA_\mathrm{w}(T(t) - T_a(t))}{WC_\mathrm{w}} \tag{3}$$

$R$ denotes the resistance of the nitinol wire, $W$ the weight of the wire, $C_\mathrm{w}$ the specific heat coefficient of the wire, $h$ represents the convection heat coefficient of nitinol, and $A_\mathrm{w}$ represents the transverse area of the wire. An approximation, shown in Eqs. 4 and 5, which considered the addition of simple and continuous functions, was used to describe the force and shape functions

$$F(r) = \sum_{i=1}^{n} f_i(r) \tag{4}$$

$$f(r) = \frac{a}{1 + e^{-b(r-d)}} + c \tag{5}$$

$a$ determines the lower bound, $c$ denotes the upper bound for the sigmoid, $b$ denotes the slope, and $d$ translates the sigmoid over the $r$ axis. The parameters were obtained from a first set of experiments. A comparison with later set of experiments, which were used to validate the model, showed a 0.95 correlation. Later, Wang et al. (2019a) presented their work on predicting the thermomechanical

training behavior of the SMA devices. Their work came out of the need to have a model to describe the complex SMA devices under complex thermomechanical loading paths. They developed the model based on an earlier established constitutive model and an efficient numerical algorithm (Wang et al. 2017). Validation with experiments showed that the numerical results from the FE simulation well described the thermomechanical training behavior of the SMA wave spring actuator.

### Studies on the numerical modeling of SMAs

Most of the commercial and academic finite element softwares used for modeling SMAs utilize the implicit integration schemes. The trouble with this is that the implicit integration schemes are impractical for addressing complex cases like in high-speed/nonlinear dynamic analyses, or in fully coupled thermomechanical dynamic analyses. These kind of complex phenomenon are in several SMA applications. To solve this problem, Scalet et al. (2017) proposed an explicit integral scheme for the three-dimensional phenomenological model called the Souza–Auricchio model (Souza et al. 1998; Auricchio and Petrini 2004)—which represents both the pseudoelastic and shape memory behavior. Several complex boundary value problems were tested with the proposed algorithm.

With the aim of providing an improved finite element simulation method for structures with ferromagnetic shape memory alloy (FSMA), Jafarzadeh and Kadkhodaei (2017) enhanced a previously developed constitutive model (Shirani and Kadkhodaei 2014, 2015) with experimental observations. The previously developed model explained the behavior of a single crystal FSMA (of tetragonal lattice structure) that had two martensitic variations (Variant 1 and Variant 2). The different variants are shown in Fig. 4, where the variants are denoted according to the orientation of their magnetization (in relation to the coordinate system), i.e., if the magnetization of a variant is in $x$-direction, then it is Variant 1, and similarly for $y$ and $z$ as Variant 2 and Variant 3. The equations for the model were given by the following expressions.

$$\varepsilon_x = S(\xi)\sigma_x + \xi\varepsilon^{r,\max} \tag{6}$$

$$S(\xi) = (1-\xi)S^{V1} + \xi S^{V2} \tag{7}$$

$\sigma_x$ and $\varepsilon_x$ are the stress and strain in $x$-direction. $S(\xi)$, $S^{V1}$, and $S^{V2}$ are the total compliance value, compliance value of Variant 1, and the compliance value of Variant 2. $\xi$ is the Variant 2 volumetric fraction, and $\varepsilon^{r,\max}$ is the absolute value of the maximum reorientation strain. Based on a proposed phase diagram, the model predicted the stress–strain response under compressive loading/unloading cycles (for a constant perpendicularly applied magnetic field). This earlier model, however, was not well fitted to describe magneto-controlled loadings. Hence, this article was focused on enhancing the previous model, to describe both mechanical and magneto-mechanical loadings. This was done by the phenomenological enhancement of the phase diagram of the FSMA. Firstly, the phase diagram included a stress-induced reorientation region (SIRR), wherein the limiting magnetic field varied with applied compression. Secondly, two boundaries for reverse reorientation initiation—one active during the mechanical loadings at constant magnetic fields, and the other accounted during the magneto-controlled loadings—were considered. All of this had been incorporated into a subroutine, to be used in the ABAQUS solver software. The proposed model, and the accompanying simulation method, was tested by simulating a spring actuator and comparing its results with experimental results.

For simulating the SMAs in the pseudoelastic range, using the Zaki–Moumni model, Gu et al. (2017) presented a numerical implementation of the large time increment (LATIN). This was proposed primarily to address the convergence issue faced in cases where phase transformation process presents only a little or no hardening—

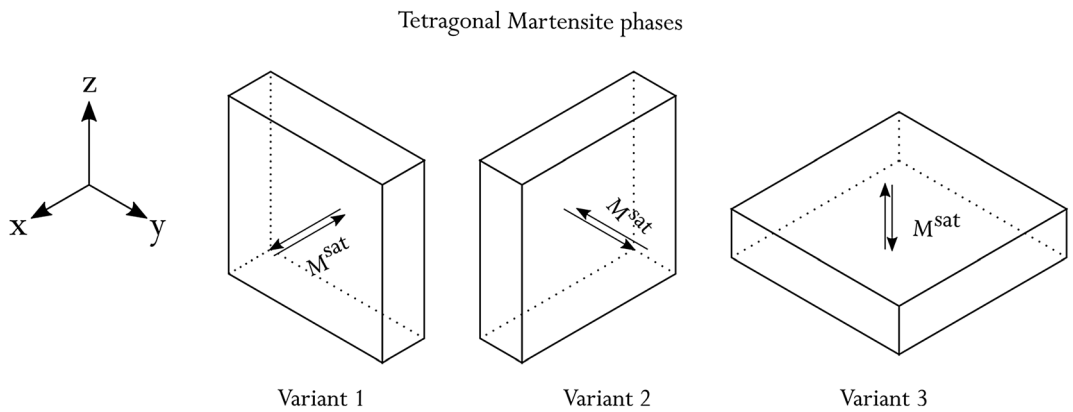


**Fig. 4** The three martensite variants and their magnetization vectors, adapted from Lagoudas (2008)

where a small stress variation in load increment leads to large variations in strain and local state variable. The LATIN method has two stages (taking place one after the other); the first stage solution satisfies the static admissibility condition for each load increment (without the consideration of the consistency with the phase transformation conditions), and the second stage involves the determination of the increments of the local state variables for the entire loading path. Computational tests on a stent structure, which simulate SMAs with flat phase transformation plateau, are provided to showcase the ability of the proposed approach.

To study the pseudoelasticity and the shape memory effects of the SMA fiber-reinforced composite structures, Xu et al. (2018) developed a generic 3D multiscale finite element model. The constitutive behavior of the SMA, developed based on a thermodynamic model (Chemisky et al. 2011), considers three path dependent strain mechanisms. The macroscopic FE model and the microscopic FE model were implemented on the FE software ABAQUS, through its user-defined subroutine. The multiscale thermodynamic model was successfully tested and validated with two parts of examples for isothermal and thermomechanical loadings. The first part, which presented two isothermal loading examples, showed the pseudoelasticity of the SMA/epoxy composite. In the first example, a simply supported composite cube, under isothermal tension compression displacement load, was modeled by the multiscale model, and its results were compared with a fully meshed model. In the second example, the results of the multiscale model of a bending composite beam were compared and validated with the results from an earlier study (Dehaghani et al. 2017). The second part, which aimed the study of the shape memory effect, presented two thermomechanical loading cases with a tension cube and a bending beam. Owing to the generic computing platform ABAQUS, the proposed model could be employed to design and study several other SMA composite structures.

Other notable studies in this topic focus on the development of numerical models for nonlinear damping behavior of SMA in martensitic state (Haghdoust et al. 2018) and for representing fully coupled SMAs under multiaxial loadings (Hashemi et al. 2019). In the article on the nonlinear damping behavior of SMA (Haghdoust et al. 2018), the goal was to model the amplitude-dependent damping of the martensitic phase of the SMA. Prior to this work, the models for martensitic-state-damping were not accurate in describing the observed experimental behavior, and the existing techniques usually used a linear assumption. In this article, the materials' hysteresis behavior is modeled to in turn model the nonlinear damping. To model the low strain range, martensitic-state SMA's hysteresis cycle, a phenomenological model, based on a modified version of Masing's rules (Masing 1926; Kramer et al. 1996), was developed. Accordingly, the following hysteresis function was proposed and used by the authors.

$$\phi = \frac{(E_{\text{av}} - E_{\text{in}})}{\varepsilon_{\max}}(\varepsilon - \varepsilon_{rev})^2 + E_{\text{in}}(\varepsilon - \varepsilon_{rev}) \tag{8}$$

$\phi$ is the hysteresis function. $E_{\text{av}}$, $E_{\text{in}}$, $\varepsilon_{\max}$ are the average elastic modulus, the initial elastic modulus, and the maximum strain of the hysteresis cycle (the hysteresis cycle with the highest amplitude). For the $Ni_{40}Ti_{50}Cu_{10}$ and $Cu_{66}Zn_{24}Al_{10}$ SMAs, this function guaranteed the observed lens shape cycle. This model was validated by comparing the numerical hysteresis cycles with the experimental hysteresis cycles. Further, the model was implemented in a user subroutine of the ABAQUS FE Code to obtain the free response of the hybrid composite encastred beams. Again, the successful validation of the amplitude-dependent damping of the beams confirmed the model's effectiveness in describing the behavior of complex hybrid composite structures. In the article on studying SMAs under multiaxial loadings (Hashemi et al. 2019), the authors present a fully coupled 3D rate dependent model for the SMA. All of the existing studies on SMA with multiaxial loadings have either been solved like 1D cases or have been proposed exclusively for pseudoelastic response. Additionally, these studies have been studied for specific geometries, and not much attention has been given to thermal cycles of the SMAs. Addressing all these points, the present study, as stated before, has developed a three-dimensional rate-dependent model, by extending Kadkhodaei's formulation (Alipour et al. 2015). This formulation is implemented into the ABAQUS FE Code by user-defined material subroutine. The presented model was able to simulate both the shape memory effect and the pseudoelasticity, for strain rates ranging from quasi-static to high-rate loadings. Additionally, it was capable of modeling SMA components with any geometry (and boundary conditions) for both mechanical and thermal loading. All of this were validated by comparing the numerical results of different SMA structures (SMA wires, thin-walled tubes, and helical springs), against the experimental, analytical, and numerical studies found in the literature.

### Porous shape memory alloys

Owing to their potential for applications in medical implant devices, and for high energy absorption structural materials, the porous shape memory alloys (PSMAs) have been garnering attention in recent years. The combination of the benefits of a porous structure, with the benefits of pseudoelastic effect and the shape memory effect, is what drives the interest for various applications. As there has been significant progress in the manufacturing of

customized porous SMAs (aiming at regular distribution of voids), the necessity of analytical and numerical models, that characterize their mechanical responses, has also become important. In this regard, a computational homogenization technique, that can integrate the constitutive response of a porous SMA into a multiscale numerical procedure, was proposed by Sepe et al. (2016). To obtain accuracy with reasonable computational effort, the non-uniform transformation field analysis (NUTFA) (Sepe et al. 2013) was used to study the porous SMA. In the study, the porous SMA was viewed as a composite material with a dense SMA matrix, and the void was represented as inclusions with zero stiffness. The dense SMA was modeled based on the Souza–Auricchio model (Souza et al. 1998; Auricchio and Petrini 2004; Evangelista et al. 2009). Apart from comparison with experimental results from literature, a detailed comparison of the proposed NUTFA, with Mori–Tanaka and the uniform transformation field analysis, was done for different two-dimensional and three-dimensional problems. In the comparison studies, for the 3D geometry, two different unit cells of respective porosities of 13% and 35% were analyzed. The first study of 13% porosity was in line with the experimental study conducted on porous SMA NiTi of $f = 0.13$ ($f$ being the void volume fraction), by Zhao et al. (2005). Consequently, a comparison between the experimental results and the FE numerical results was first done to look into the effectiveness of the proposed procedure. Figure 5a shows the results of the homogenization methods (the Mori–Tanaka, UTFA, and NUTFA), the nonlinear micromechanical FE response, and the experimental curve, for the porous NiTi SMA, subjected to the compressive average strain history.

Here, it can be seen that the FE results provide the closest approximation to the experimental curve. With the Mori–Tanaka technique, in the last part of the loading phase, there is an underestimation of the maximum average stress. The UTFA, though gives a good approximation of the FE result, it does overestimate the phase transformation activation stress. The NUTFA, on the other hand, very closely matches the FE curve, and subsequently also matches the experimental curves in the same manner as the FE curve. In a similar second study, with 35% porosity, shown in Fig. 5b, the NUTFA procedure is again able to produce the FE results accurately. Thus, both these plots demonstrate the accuracy of the homogenization technique in predicting the 3D behavior of the porous SMA material. Studies for 2D case showed that the Mori–Tanaka and UTFA approaches did not deliver an accurate prediction as that of the NUTFA technique.

In terms of applications, the good biocompatibility, corrosion resistance, and the similar mechanical properties to body tissues, of the porous NiTi have led them to be an apt candidate for bone scaffolds. Besides the above mentioned advantages, the interconnected pores of the microstructure of bone scaffold facilitate another function, namely the transportation of body fluids between body tissues. While designing the PSMA, in order to obtain proper function, the mechanical properties of the scaffold must be tailored similar to that of the bone. As the fabrication and characterization are both expensive and time-consuming, the necessity of a reliable numerical approach,

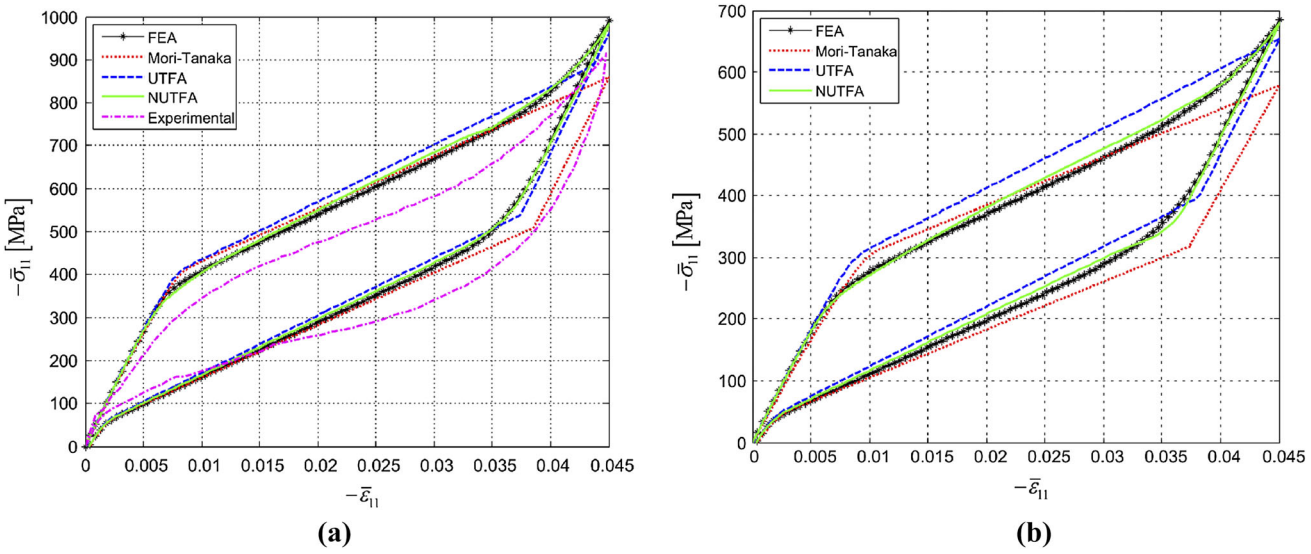


**Fig. 5** The average compressive stress versus the average compressive strain plots of, **a** the homogenization, FE, and experimental curves for 3D unit cell of porous NiTi for $f = 0.13$, **b** the homogenization, FE curves for 3D unit cell of porous NiTi with $f = 0.35$, with permission from Springer Nature (Sepe et al. 2016)

to predict the response of the PSMA, is indispensable. For this, a two step mesoscale finite element model was developed by Karamooz-Ravari and Shahriari (2018). First, to designate the bulk material of PSMA, based on the microplane theory, a 3D constitutive model of dense SMA is formulated. Then, the geometric model is developed with Voronoi tessellation of 3D space. The mechanically and geometrically periodic boundary conditions are applied to the model. In addition to validating the model with experimental results from the literature, the effects of other associated phenomenon like the number of cells, the level of randomness, and the applied boundary conditions, on the stress strain response, were also analyzed.

Another notable study in the PSMA, by Abdollahzadeh et al. (2019), presents the development of the numerical procedure for modeling of superelastic behavior of PSMA at different levels of pore volume fraction. Just as in the first mentioned study, the PSMA was simulated with dense SMA matrix elements, but the pores were represented as randomly distributed elements characterized by near-zero stiffness. To describe the SMA matrix, the Boyd and Lagoudas (1996) and Lecce et al. (2014) plasticity-like phenomenological model was used. In the paper, a homogenized FE model was established with the incorporation of the effective Young's modulus and the modification of phase transformation function into the constitutive equation. Here, the relation of the Young's modulus, to the pore volume fraction is linear, while that of the phase transformation function is quadratic. Though the numerical tests show that the model is precise, and method is computationally effective, there is the drawback (that has been stated by the authors)—the method just cannot model PSMA with pore volume fraction greater than 50%.

### SMA actuators

While the SMA wires, ropes, and bars are relatively well-known forms (that have been researched for various applications), the SMA Belleville washer is a new mechanical component, that is starting to gain popularity for its features and potential applications. As can be guessed, it has an annular shape, which facilitates an even and concentric force transmission, which subsequently leads to larger stability than other springs. Additionally, it is endowed with self-recovery and hysteretic damping due to its superelastic ability. Though it was initially utilized in electric circuit stabilization, avenues are now opening in civil engineering—to be employed as seismic resisting dampers. In this application context, researchers have started analyzing many of its characteristics. One such work is the study by Fang et al. (2016), wherein the mechanical properties of the washers were analyzed by a series of experimental studies, with different stack combinations, and under varying temperatures and loading. In the tests conducted at 10 °C and 23 °C, the washers displayed good self-centering and energy dissipation capacities. Though slight degradations of the hysteretic responses were induced in a few cycles, the hysteretic loops were stabilized after that. In addition to this, the washers also showed good flexibility in load resistance and deformation. In addition to the experimental studies, numerical studies were also conducted to further investigate the washers. Based on these studies, a phenomenological model was developed. Though the 3D constitutive models could offer a detailed description of the deformations and stress conditions in the washer, the uncertainties of the SMA material behavior (caused due to the effects of fabrication process, heat treatment, and material degradation) also need to be addressed. For this reason, the use of a test-validated 1D model, which directly accounts the macro-hysteretic responses of the SMA washers, is preferred by civil and seismic engineers. In the proposed constitutive model, two parameters which varied with increasing loading cycles—the forward transformation start force and the residual displacement—were only considered as loading history related variables (as the rest could be obtained from the test data). With this, the simulation results for the load-deformation response were close to the experimental observations.

Using SMA, an actuator with long stroke and constant force can be obtained with the Rolamite architecture. The Rolamite, invented by D Wilkes in 1967 at the Sandia National Labs (Eulert 1969), is a roller strip mechanism, wherein two rollers, with an entwining S-shaped metal strip, are mounted between two parallel fixed guides. The Rolamite can roll back and forth with much ease, as the design facilitates a very low friction coefficient (even with preloads), even without lubrication. Spaggiari and Dragoni (2017) proposed the idea of employing the SMA as Rolamite power element, to use its SME to change the elastic properties of the metal strip, to provide actuation force. Compared to the SMA wires and springs, this would have an even longer stroke and near constant force–displacement characteristics. An analytical model was proposed to describe the behavior of the SMA Rolamite as a function of strip geometry. For SMA material, the austenitic phase is incorporated as linearly elastic, while the martensitic phase is described with a simple interpolating function (Spaggiari and Dragoni 2014; Spaggiari et al. 2015).

### New constitutive models and modeling of SMA structures

Usually, in analytical modeling of the SMA beams, for either pure bending or bending due to tip loading, researchers solve for the bending during the loading process. And, these models do not sufficiently describe the

evolution of phase transformations during the unloading process. In this regard, the study by Van Viet et al. (2018) offered an analytical model, for the bending of a cantilever superelastic prismatic SMA beam, subjected to a concentrated tip force, considering both the loading–unloading cycle. The analytical model was derived from the Zaki–Moumni model (Zaki and Moumni 2007), with Timoshenko beam theory—which was also a step up from the previous studies, which used Euler–Bernoulli beam theory. The moment–curvature and shear force–shear strain relations, apart from representing loading and unloading, also accounted for the nonlinear stress distribution in the mixed austenite and martensite phase regions. The model presented a detailed description of the unloading process and also presented the influence of martensite volume fraction on the effective stiffness of phase mixture regions. Finally, the analytical model was validated with numerical results from 3D finite element analysis.

As far as constitutive models for SMAs are concerned, there are quite a few models based on the infinitesimal strain theory (for describing small deformations). However, SMAs do undergo large strains, reversibly deforming upto 8%, and also in certain applications, may undergo large rotations. To address this, there have been attempts, based on a finite deformation framework, to develop constitutive models. One such recent attempt is the study by Xu et al. (2019), wherein three important phase transformation characteristics, which have not been addressed in the previous studies, were considered while developing the model for polycrystalline SMAs. These three characteristics were (i) the smooth transition during phase deformations, (ii) the stress-dependent transformation of strain, which would account for the coexistence of oriented/self-accommodated martensitic variants, and (iii) a stress-dependent critical driving force, to relate the applied stress to the size of hysteresis loop. Taking on from an earlier study on developing an infinitesimal SMA model (Lagoudas et al. 2012), this work developed the model by the standard Coleman–Noll procedure with the classical thermodynamic laws. The material response of the SMA was imbibed by choosing the scalar martensitic volume fraction, and the second-order transformation strain tensor, as internal state variables. The developed finite strain SMA model, using logarithmic strain and logarithmic rate, accounted for the large strains and rotations. The formulation was used to analyze SMA bar, SMA beam, SMA torque tube, and a SMA flexible structure under stress or thermal loadings, and the results were further compared to those obtained from ABAQUS solver. In similar lines, the article by Yu et al. (2018) also focuses on constructing a constitutive model for polycrystalline NiTi SMAs. But unlike the previous study, the theme here was to describe the grain size-dependent deformation of the SMAs, from microscopic scale (by a nonlocal model) to the macroscopic scale (by a local one). The model itself is derived from an earlier nonlocal model (Qiao et al. 2011), with an energy-equivalent rule, which equalizes the macroscopic local model and the microscopic nonlocal one, in terms of both energy and dissipation.

In another study focusing on polycrystalline SMAs, Rizzello et al. (2018) developed a novel, physics-based dynamic model for 1D polycrystalline SMA wires (used for actuation and sensing purposes). While the model was developed by extending the one developed by Heintze et al. (2004), which in turn was based on Müller–Achenbach–Seelecke (MAS) model for single crystal alloys, it did have some shortcomings. As listed out by the authors, these limitations are: not explicitly accounting for the temperature-dependent hysteresis, not incorporating the actuation and sensing behavior, and restricting the model to superelastic SMAs. All of these were addressed in the newly developed model, wherein in addition to temperature dependency, the stress–strain and resistance-strain characteristics of the SMA wires were also described. The model adopts the single crystal notion, due to which the complex nature of the polycrystalline SMA wire is expressed in a computationally efficient fashion. The simulation time itself is comparable to the single crystal SMA models. For validation of the proposed model, experiments were conducted on a superelastic NiTi wire and a quasi-plastic NiTi wire. The comparison showed that the model was able to exactly reproduce the various experimental hystereses curves.

In the topic of modeling SMA wires, in relation to applications, the study by Lambert et al. (2017) has to be mentioned. As with any material, there are both benefits and disadvantages associated with the SMA actuators, and both of these must be incorporated into the models when trying to get a realistic representation in applications. In their study, the authors developed a general platform, which can be used for design and analysis of SMA actuators in complex mechanical systems, considering the above stated point. To state explicitly, for describing an actuator incorporated in a multibody dynamic system, the thermo-electro-mechanical constitutive models of the SMA were implemented in a multibody dynamics software. In a specific case of a working ball-on-a-beam setup, where the ball position was controlled by regulating the current passed through the SMA wire, this model was used in conjunction with the sliding mode control.

## Applications of shape memory alloys

This section targets the foremost applications of SMAs in recent times. The realm of construction, biomedical, aerospace, and offshore form the main areas. For the sake

of completeness and to stay connected with the available literature on SMAs, the accomplished review works, performed before, in the applicative domains of construction (DesRoches and Smith 2004; Wilson and Wesolowsky 2005; Song et al. 2006; Alam et al. 2007; Qian et al. 2010; Ozbulut et al. 2011; Alvandi and Ghassemieh 2014; Cladera et al. 2014), biomedical (Petrini and Migliavacca 2011), aerospace (Wang and Wu 2011), and offshore (Song et al. 2010) have also been incorporated in this article. This way, the readers of this article can have an overview on the progression of development and application of SMAs.

## Shape memory alloys in construction sector

### Crux of former reviews

A critical review on the utilization of shape memory alloys in construction sectors was undertaken by Chang and Araki (2016)—this is the latest available review article in the open literature till date. Their review work (and the scientific articles cited therein) gave an overview of the progress and development of SMAs in construction domain. Specifically, their review article provided a glimpse on the potential and the limitations of shape memory alloys in construction. This was supplemented by discussions concerning the use of shape memory alloys to (1) eliminate the impact of natural disasters, (2) enhance structural performance, (3) diminish vibrations by stepping up damping, and (4) integrate the SMAs into civil structures to respond to the environmental circumstances and enhance energy efficiency. The factors affecting the SMAs pertaining to their applicability in construction were also outlined. It was pointed out that SMAs have been successfully employed in industrial sectors owing to their inherent characteristics of superelasticity, shape memory effect, and high damping, although their applicability in construction sectors has not been well explored due to the cost limitations (as materials are required in large scale), availability of affordable SMAs with high performance and temperature-dependent behavior.

Motivated by the fact that SMAs can act as reinforcement material, by offering large recoverable deformations (self-centering ability) and by enhancing the ductility of reinforced concrete, Shajil et al. (2016) reported experimental analysis for evaluating the self-centering ability and ductility of beams and beam–column joint by involving randomly distributed pseudoelastic shape memory alloy (PESMA) fibers. From the three point loading experiments on beam–column joint specimens incorporating steel and PESMA fibers, they concluded that the ductility and self-centering ability of composite, with PESMA (NiTi) fibers, was more superior than steel fibers. The experimental results indicated that by the use of NiTi fiber (0.5% by volume) in the cement mortar, 40% or more of the deformation was recovered (i.e., self-centering factor was more than 0.40), whereas the same factor for the case of steel fiber (0.5% by volume) was nearly 0.10 only. Moreover, the ductility factor (measure of the rate of delay between the yield and the damage of the structure) was also found to be very high (nearly 5) for NiTi (when used as randomly distributed fibers in cement mortar beams), while the ductility factor for steel fiber-reinforced beams was having a lower value (nearly 2.5). It was also reported that energy dissipation and fracture toughness can be enhanced significantly by the utilization of randomly distributed NiTi fibers as secondary reinforcement in concrete structures (which are prone to large deformation during cyclic loading).

Focusing on the lightweight, high strength, and high corrosion resistance properties of fiber-reinforced polymer (FRP) composites and relying on the notions that SMAs possess excellent corrosion resistance, better energy dissipation potential, and high fatigue properties, Daghash and Ozbulut (2016) performed characterization of superelastic shape memory alloy fiber-reinforced polymer composites under tensile cyclic loading. In particular, the composite comprised of thermoset epoxy matrix, which was reinforced with superelastic SMA wires. Under constant cyclic load for 100 cycles, two specimens with 4.9% and 9.9% SMA fiber volume ratio were tested. The test results manifested that FRP composites reinforced with different volume ratios of SMA fibers can fully recover large strains (between 2.4% for low fiber volume ratio and 6.4% for high fiber volume ratio) upon unloading and can achieve tensile strain between 10% and 12%. For SMA-FRP with 4.9% fiber volume ratio, accumulation of residual deformations in the epoxy matrix affected the mechanical behavior, and subsequently resulted in limited recentering abilities for the composite. On the other hand, the SMA-FRP with 9.9% fiber volume ratio experienced minimal residual strains and recovered 82% of its maximum strain under cyclic loading. The fractured surfaces of failed specimen was examined by means of scanning electron microscopy (SEM) technique to understand the failure mechanism of the composite. In failed specimen, when the debonded areas increased significantly, and when the epoxy could not sustain the applied stresses, failure occurred. It was found that failure of the composite was allied with contraction of the wires at some locations, which subsequently led to debonding between the wires and the matrix. The results of the study revealed that SMA-FRP composites are capable of recovering relatively high strains upon unloading, and can display high failure strains. As an alternative to FRPs, SMA-FRPs can be utilized in near-surface-mounted applications for better strengthening of concrete structures. Kim et al. (2016) employed short

SMA fibers to cement mortar in order to come up with SMA-fiber-reinforced cement composites (SMA-FRCCs) bearing prestressing and crack closing capabilities by performing direct tensile tests after a short (10 min) heat treatment. Two types of SMA fibers (NiTi and NiTiNb alloy fibers) were added by 1.5% volume content in a mortar matrix with 55 MPa compressive strength. After heat treatment, SMA-FRCCs exhibited reduced tensile strength due to the radial cracks surrounding the expanded SMA fibers. Moreover, owing to shape memory effects, SMA-FRCCs successfully displayed their prestressing capability after heat treatment. The study also manifested that the heat treatment steps up Young's modulus of SMA-FRCCs in tension because of shape memory effects. In addition to this, they stressed on the need to analyze the temperature of SMA fibers embedded in a mortar matrix and further pointed toward the necessity of novel methods to activate shape memory effects.

To withstand lateral loads, structures require components holding potential to securely shift these loads to the foundation. The behavior of concrete shear walls becomes crucial in overall performance of the structures, as they need to dissipate the lateral loads acting on the structures. Considering these aspects, Ghassemieh et al. (2017) depicted the impact of SMAs within the coupling beams of the shear walls by employing finite element method. This study was carried out to assess the effectiveness of superelastic behavior of SMA in decreasing the damage to the coupled shear walls, as compared to the conventional steel rebars. The study revealed that in contrast to diagonal steel rebars, involving diagonal SMAs in coupling beams and opening corners can lead to effective reduction of damage (due to the high yielding strain characteristic of SMAs). The flexural behavior of reinforced concrete beams, strengthened and prestressed with iron-based SMA (Fe-SMA) strips, was delineated by Shahverdi et al. (2016). As an outcome of the study, the cracking loads and mid-span deflections of prestressed beams, when compared to other beams, were found to be higher and lower, respectively. Better strengthening effects were achieved in near surface mounted Fe-SMA (NSM Fe-SMA) strengthened beams, which showed that involvement of NSM Fe-SMA strips worked well as prestressing elements in concrete beams. The results of the study showed that the cracking load of the beam (strengthened with prestressed Fe-SMA strips) was on an average 80% higher than the cracking load of the beam (strengthened with the same Fe-SMA in the absence of prestressing). It was also pointed out that in comparison to non-prestressed beam (with the same amount of Fe-SMA strengthening), the displacement at a load of 8 kN was observed to be 75% less for the prestressed beam. As concluded by the study, some advantages that prestressing offered were reduced crack widths, reduced deflections, reduced stress, and increased fatigue resistance. The utilization of superelastic SMA bars in NSM strengthening applications can lead to certain advantageous features like improved bond behavior, enhanced deformation capacity, and post-event functionality. Following these attributes, Daghash and Ozbulut (2017) studied the bond–slip behavior of superelastic SMA bars—which can be brought into effect as strengthening reinforcement in NSM strengthening. The study indicated that sandblasted SMA bars manifested quite good bond behavior when used with the correct filling material in NSM strengthening applications, and the mechanical anchorage of SMA bars substantially stepped up the bond resistance. Since the high cost of NiTi SMAs hampers the utilization of SMAs in civil structures, they also stressed on the importance of cost-effective SMAs. These cost-effective SMAs can actively encourage the widespread use of SMAs as NSM reinforcement for strengthening concrete members. Figure 6 depicts the NSM strengthening of a RC column by means of superelastic SMA bars.

Moving ahead with the further progress, Rojob and El-Hacha (2017) applied self-prestressing technique using iron-based SMA bars for flexural strengthening of reinforced concrete beams. At the tension side of the reinforced concrete beam (2000 × 305 × 150 mm), the prestrained Fe-SMA bar was anchored inside a precut groove. The bar was activated through heating (above 300 °C) which induced prestressing force in the bar. A prominent increment in the yielding and ultimate load capacities was reported through this study. The ductility of the beam was remarkably enhanced because of the yielding nature of Fe-SMA material, unlike the prestressed FRP strengthening

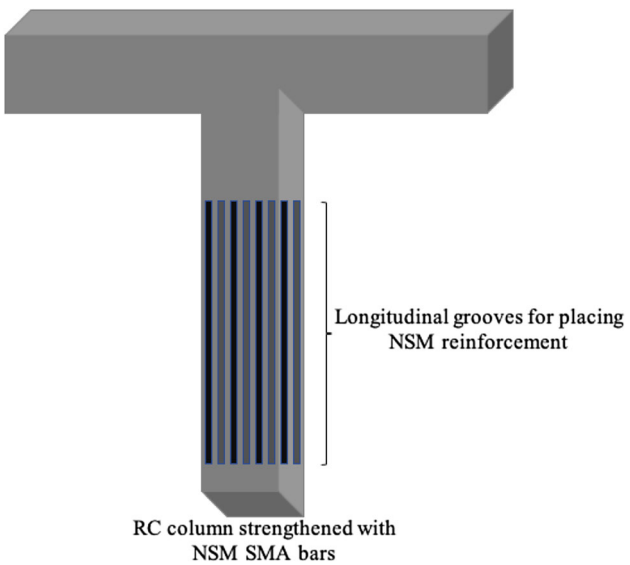


**Fig. 6** Utilization of superelastic SMA bars in NSM strengthening, adapted from Daghash and Ozbulut (2017)

techniques. It was pointed out that the ease of employing prestressing force, and the ductility of Fe-SMA material provided an upper hand to self-prestressing technique (obtained using Fe-SMAs), over the prestressing technique (obtained using FRPs). As highlighted by the authors, there was no solid conclusion drawn on the effectiveness of the thermomechanical training of the Fe-SMA due to the anchorage setting (during the heating process and bending test). Also, a relaxation of Fe-SMA bar and consequently a reduction in the prestressing force were noticed because of the anchorage setting. From the viewpoint of future research, they also stressed to work on reinforced concrete beams subjected to freezing and thawing cycles under sustained loading. The performance of an 8-mm-diameter Ni–Ti SMA cable for its utilization in reinforced concrete application was depicted by Mas et al. (2017). As an outgrowth of the study, it was manifested that, due to its good superelastic properties, the cable possessed huge possibilities with only a marginal permanent strain ratcheting (less than 1% over fifty large strain cycles). It was also reported that the low modulus of elasticity of the SMA cables (considered in the study) proved to be a handicap for its application in reinforced concrete members. Hence, it was suggested to increase the modulus of elasticity by tuning the alloy or by heat treatment process in order to (1) lower the transformation temperature, (2) avoid the excessive longitudinal and transverse deformations, and (3) enhance the bonding properties. Furthermore, they also highlighted the prospect of utilizing Ni–Ti cables in non-bonded applications and/or in post-tensioning solutions, to pave way for new possibilities to the structural concrete industry. Santos and Nunes (2018) addressed the dynamic response of a novel adaptive vibration control device, with frequency self-tuning capabilities, based on the temperature modulation of SMA restitution elements. By using numerical models of a lively footbridge, they performed simulations to provide an insight into the high potential of this adaptive control approach in the reduction of vibrations in civil engineering structures. The use of active SMA cables in the undertaken system offered a viable design solution to diminish the structural acceleration arising due to pedestrian loading in footbridges.

Because of their carbon storage capacities, flooring materials can extend their helping hands in construction regime as they are lightweight, pre-fabricated and environment friendly. Drawing on this, Huang and Chang (2018) conducted a study, using numerical simulations (on OpenSees software) to assess the effectiveness of SMA-based semi-active tuned mass damper in a real-scale timber floor. They considered free vibration and human footfall-induced vibration as inputs. Their study revealed that retuning using SMAs can effectively decrease the structural response at a large range of frequencies, thus resulting in the attenuation of the footfall-induced vibration. Counting on aging, corrosion and lack of sufficient load carrying capacity, steel structures these days require strengthening. In view of this Izadi et al. (2018) presented the development of an Fe-SMA system for the strengthening of steel plates by utilizing SME for prestressing the steel plates. The proposed strengthening technique was capable of removing the hindrance linked with conventional prestressing, for instance hydraulic jacks, and also imparts a fast installation strategy because it does not need any surface preparation or curing for bond application. By bringing in microcapsules and SMAs into play, Bonilla et al. (2017) worked on the evaluation of dual self-healing mechanisms in concrete. In particular, their objectives were inclined toward, firstly, to analyze self-healing effectiveness of calcium nitrate microcapsules in steel and SMA reinforced-concrete beams, secondly, to examine the structural behavior and stiffness recovery of beams after damage, and lastly, to depict the impact of SME on self-healing potentials of concrete beams. Their study featured the fact that, under high stress circumstances, microcapsules possessing calcium nitrate would get fragmented and subsequently discharge healing agents during crack formation. Further, to replace conventional structural steel reinforcement, they used SMAs triggered by induced heat. The entire process binds together the crack interfaces permitting the microcapsules to heal the concrete material. Liu et al. (2018) proposed the application of superelastic SMA strands for improving the seismic performance of unbonded prestressed reinforced concrete (RC) bridge column. RC column, RC column with unbonded prestressing steel strands (UBPS column), and UBPS-SMA column were considered by them in the study. In order to compare and reveal the seismic response of these three types of columns, for a continuous box girder bridge, they involved quasi-static and seismic analysis. The study resulted in enhancing the self-centering capability of column under the requirement of increasing the prestressing force ratio and the maximum tensile force ratio.

Owing to the SME, SMAs in the form of bars and strips can be employed as prestressing elements in new RC members and also for strengthening existing RC structures. Propelled by this, Shahverdi et al. (2018) developed a cost effective Fe-SMA for application in civil engineering structures. Fe-SMAs are less expensive than nickel–titanium (NiTi) SMAs because (1) of their low cost of raw materials, (2) they can be manufactured easily, (3) they can be produced on an industrial scale at atmospheric conditions without expensive and high-vacuum processing facility, (4) they can be activated at distinct temperatures (100–250 °C) by resistive heating over a short period (about 1 min) of time, and (5) they can be manufactured in different shapes (for instance, ribbed bars or strips) by

means of hot and/or cold forming. In addition to the low material cost and ease of manufacturing, compared to NiTi, the Fe-SMA also exhibits high tensile strength, excellent shape recovery stress, and high elastic stiffness. Their study revealed the experimentally determined characteristics along with the measured recovery stress and strain of Fe-SMA strips. The tensile strength of about 1000 MPa with a corresponding strain at failure of more than 40% was reported in the study. Moreover, after heating the Fe-SMA strips to 160 °C, recovery stresses of 300–350 MPa were noted. Furthermore, during the heating/cooling cycle of the 1.5 mm thick strip to/from a temperature of 160 °C, recovery strains of 0.15–0.40% were figured out. It was also stated that Fe-SMA strips can be implemented as external end-fixed reinforcements to strengthen RC structures. Wang et al. (2019b) provided a novel precast RC wall system, involving SMA bars and replaceable energy dissipating devices, to attain earthquake resilience. This structural system offered major advantages such as the self-centering capability (imparted by unbonded superelastic SMA bars, which are employed in the bottom boundary zones of the wall), concentrated energy dissipation and damage in the replaceable steel angles, and an earthquake resilient design (which needed minimal repair even after strong earthquakes). Their proposed SMA-based RC walls, as compared to conventional RC walls, bestowed a promising solution for high-performance structural systems, which are demanded by modern resilient and sustainable civil infrastructure.

Ghafoori et al. (2019) provided the first methodical study on the structural fire behavior of prestressed Fe-SMA members (which are used in pioneering retrofits of concrete slabs). Figure 7 exhibits Fe-SMA members that are linked to concrete slabs using a layer of either shotcrete (Fig. 7a) or an end anchorage system (Fig. 7b).

In order to predict the fire-induced prestress loss in Fe-SMA members of retrofitted civil structures, a simple engineering model was developed by them. When applied to a shotcrete-embedded prestressed Fe-SMA member, a two-stage prestress loss-temperature relation was predicted through this model. It was pointed out that the prestress loss is almost linear up to a temperature of approximately 270 °C in the first stage (due to the thermal expansion of the material). In the second stage, the rate of the prestress loss stepped up significantly after exceeding 270 °C (due to the onset of marked plasticity). It was also observed that at approximately 320 °C, the prestressing of the Fe-SMA rebars (with a concrete cover of 20 mm) fully disappeared after 20 min. Further, it was concluded that the time of the total prestress loss can be lagged by the use of (1) thicker shotcrete cover and (2) protective thermal insulation material. Izadi et al. (2019) demonstrated the use of the prestressed Fe-SMA strips to retrofit fatigue-cracked riveted connections in steel bridges. The retrofit system incorporated prestressed Fe-SMA strips that connect the top flanges of the two stringers on the sides of the connection. The Fe-SMA strips were prestressed (activated) to a maximum temperature of 260 °C. A test setup was designed to investigate the SMA-strengthened cracked double-angle connections. Further, two high cycle fatigue (HCF) tests were conducted on a pre-cracked connection. The pre-cracked connection with no strengthening was subjected to fatigue loading. After $2 \times 10^6$ load cycles, the crack propagates up to 50% of the connection depth, and because of the reduction in connection rigidity, the fatigue crack growth rate gradually decreases. Thereafter, the SMA-strengthened connection was subjected to HCF loading. It was found that for a maximum static load of 75 kN (equivalent to the maximum load in the fatigue test), the rotational stiffness of the connection is 6305 kNm/rad,

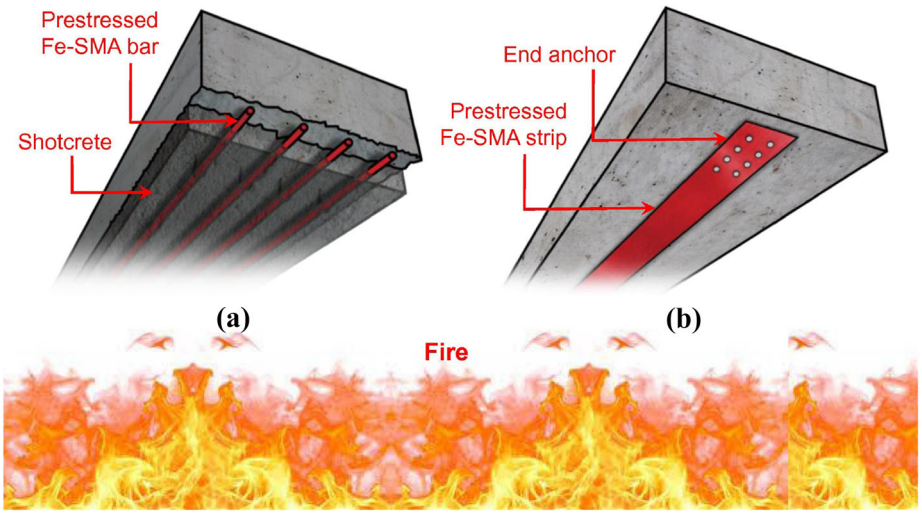


**Fig. 7** Schematic view of concrete slabs strengthened by prestressed, **a** Fe-SMA bars, **b** Fe-SMA strips exposed to fire, with permission from Elsevier (Ghafoori et al. 2019)

which resulted in a stringer-end moment of 15.5 kNm. In the flat prestressed unbonded retrofit (FPUR) system, the use of prestressed Fe-SMA strips led to crack arrest at the top of the connection. Finally, it was concluded that the stringer end moment of the connection (or out-of-plane connection deformation), which was responsible for fatigue cracking, gets diminished substantially after strengthening. Hence, by means of prestressed Fe-SMA strips, it was observed that the fatigue life was significantly improved, and the fatigue crack got arrested.

As an alternative strengthening method, retrofitting of RC members by near surface mounted reinforcement is being successfully taken into consideration nowadays due to the improvement in the load carrying capacity during service, and better use of the strengthening material capabilities. Driven by this, Abouali et al. (2019) developed a 3D nonlinear finite element model in ABAQUS to explore the strengthening of RC beams in flexure, with NSM Fe-SMA reinforcements. They preferred Fe-SMAs, since these are cost effective SMAs, and can be easily prestressed. The results of the study signified that with a low steel reinforcement ratio, NSM Fe-SMA strengthening of a concrete beam (either prestressed or unprestressed) led to the enhancement of stiffness and the rise (more than 60%) in the load carrying capacity. Rad et al. (2019) probabilistically analyzed the seismic performance of two prevalent lateral load-resisting systems viz. moment resisting frame and eccentric braced frame. They were equipped with superelastic SMA bolts in their beam–column connections and link-beam connections, respectively. Based on the results, it was noted that using SMA connections in smart buildings could significantly decrease the economic loss, by prominently controlling the undesirable residual deformations in structural fuses (because of their induced recentering behavior). The shear strengthening of existing structures is usually needed, as shear failures in RC members are linked with brittle collapses—which eventually lead to sudden material and human losses. Following this fact, Rius et al. (2019) presented an innovative system for retrofitting shear critical RC beams by using SMAs as active external reinforcement. A rectangular cross section (80 mm wide and 150 mm deep) RC beams strengthened in shear, by employing Ni–Ti–Nb SMA wires (3 mm diameter), was experimentally setup. The experimental results of the study displayed an increment of 92% in the shear strength of the retrofitted beams. It was reported that less amount of Ni–Ti–Nb SMA is required for strengthening of civil infrastructures, and such material can be placed in critical regions of the beams (despite the high cost of Ni–Ti–Nb SMA).

## Shape memory alloys in biomedical domain

### Essence of earlier reviews

Shape memory alloys have been frequently utilized in a wide range of biomedical regime. Innovative techniques are being developed to come up with enhanced biomedical devices for providing better medical facilities and treatments. The work by Zainal et al. (2015) provides an overview of the fabrication and manufacturing technique of thin-film and bulk micromachined SMAs. The review presented by them gives information about the development of SMA-based microscale biomedical devices. The review also describes the application and micromechanism for thin-film and bulk SMA. NiTi SMAs display high ductility, good biological compatibility as well as excellent corrosion and wear resistance—all of which make them cynosure, especially in the field of laser additive manufacturing (AM). Selective laser melting and laser metal deposition are usually used as laser AM techniques for fabricating complex shapes with NiTi SMAs. In their article, Dadbakhsh et al. (2016) provided an extensive review on the laser additive manufacturing of bulk and porous NiTi SMAs, starting from processes to potential biomedical applications. They also described significant areas of applying laser AM technique in order to fabricate NiTi components for medical applications. Moreover, Kapoor (2017) reviewed the discovery, material properties, processing methods, and medical applications of Nitinol SMA—with special attention to stents for the treatment of arterial diseases. The properties of this alloy offered minimally invasive surgery as well as implants to enhance life quality of millions of people. Yuan et al. (2018) reviewed the recent progresses specifically made on porous NiTi, and Ni-free SMAs for hard tissue replacements. In this review, the focus was on two aspects. Firstly, the synthesis of porous SMAs with optimal porous structure, microstructure, mechanical, and biological properties. Secondly, surface modifications which are designed to create bio-inert or bio-active surfaces with low Ni releasing and high biocompatibility for porous NiTi SMAs. Lately, Nematollahi et al. (2019) presented a review on application of NiTi in assistive and rehabilitation devices. Further, they also provided SMA applications for neurological and neuromuscular rehabilitation. This article is the recent available review in the biomedical regime involving SMA. Since aforementioned review articles are directed toward one or other aspects of SMAs, an attempt has been made to present an up to date, comprehensive overview, of distinct aspects of various SMAs utilized in biomedical domain.

In biomedical domain, SMAs have been used for the development of novel devices and therapies for

neurological conditions. By monitoring patients in the subacute phase, after a neurological lesion, Pittaccio et al. (2015) came up with a mobilizer for the ankle joint, which was designed to offer passive exercise to the paretic lower limb. They discussed distinct applications in the clinical management of upper motor neuron lesions patients, where SMA was successful in imparting additional functionality, enhancing tolerability, and allowing customization. A lot of cancer interventions nowadays are carried out percutaneously by incorporating needle-based procedures through skin and soft tissue. These procedures face certain challenges while aiming to achieve a precise navigation via tissue in reaching target locations. To tackle this challenge, active needles have been proposed by Konh et al. (2015), wherein actuation forces from SMA were used to assist the maneuverability and improve the accuracy of surgical needles. They proposed an active needle design using Nitinol (SMA) wires as shown in Fig. 8. With the objective of maximizing the needle tip deflection, to ensure the highest steerability of the active needle, a design optimization study was carried out. An enhanced design of the active needle was achieved, by integrating SMA features with the automated optimization schemes. The optimized design led to a maximum deflection of 45.84 mm with a 118.64 mm long SMA wire.

Due to their non-toxic elements, low elastic modulus, and stable superelasticity, porous Ti–Nb-based SMAs are showing their potential as promising implants for biomedical applications. By tuning the amount and size of space-holder particles, Lai et al. (2015) successfully regulated the pore structure, bearing porosity and pore size of the porous Ti–22Nb–6Zr alloys. These alloys with porosity in the range of 38.5–49.7% had shown mechanical properties similar to cortical bones, with elastic modulus, compressive strength, and recoverable strain in the range of 7.2–11.4 GPa, 188–422 MPa, and 2.4–2.6%, respectively. The study revealed that the alloys with larger pores displayed lower elastic modulus, whereas the alloys with smaller pores showed higher compressive strength under the same porosity. The cancellous bone, periosteum, cortical bone, articular cartilage, blood vessels, nerves, and so forth comprise the structure of human long bone, and due to their structural complexity, the replacement of damaged long bone is still a tough task in surgery. To handle the situation, Zhou et al. (2015) fabricated a NiTi SMA (bearing graded porosity) to imitate human long bone structure via a dedicated molding procedure. The outer layer (with porosity 14%) and the inner layer (with porosity 52%) of the bone-like graded NiTi alloy were seen to be coaxial with the interface (because of having a good metallurgical bonding). Furthermore, the compression strength and elastic modulus of the NiTi alloy with graded porosity were figured out as 360.6 MPa and 6.7 GPa, respectively. The fabricated SMA displayed resembling mechanical performance as human long bones and proved to be better implant candidates for the replacement of human long bone. The size and distribution of inclusions in semi-finished material are often considered in current standards, without placing much emphasis on the final biomedical devices built using NiTi SMA. Urbano et al. (2015) analyzed this subject by comparing the fatigue performances of NiTi superelastic wires with a simple bilinear model for fatigue response. 300-μm-diameter NiTi superelastic wires were rotary beam tested (RBT) at several strain levels. Fracture sections were traced out by field emission scanning electron microscopy (FESEM) for measuring the dimensions of the inclusions present at the fracture nucleation sites. The results of the study showed a strong correlation between the fatigue limit of wires and the predicted extreme values of inclusions at fracture origin.

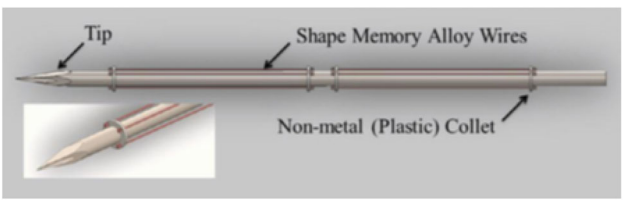


**Fig. 8** Schematic of the proposed active needle design, with permission from Elsevier (Konh et al. 2015)

The multi-functional capabilities required for medical device applications can be achieved by laser processing of SMAs. Prior to clinical implementation, the surface characterization of laser processed SMA becomes imperative in order to understand any adverse biological interaction that may occur. Motivated by this, Pequegnat et al. (2015) systematically analyzed corrosion performance, and Ni ion release performance, of a laser processed NiTi SMA, and also thoroughly characterized the surface conditions involving oxide thickness, composition, microstructure, and roughness. The contributions of this study gave an insight into the corrosion and biocompatibility performance of laser processed NiTi SMAs. The porous structure of NiTi SMAs mimics the hierarchical structure of bone, and this enables these materials to be a potential candidate for biomedical implants. Accounting on this, a porous NiTi SMA, holding a promising pore morphology and pore size, was fabricated by Abidi et al. (2015), for biomedical implant applications. The pore size and morphology can be tailored by just manipulating the characteristics of spacer powder. Porous alloys with spherical pores showed better mechanical properties than those with cuboidal pore shapes, because of the manifestation of uniform stress distribution during deformation. Aversa et al. (2016) presented an optimized system based on SMAs that can be designed by involving muscle—working as biomimetic

model. The biomechanically inspired machine (as represented by Fig. 9) discussed in their study points to antagonistic muscles pairs, that belong to the skeletal muscles which are usually systematized in opposite way (such that when one group of muscles contracts, another group relaxes). The study was directed toward providing a biomimetic model that can be utilized for a wide range of adaptive applications (switchable windows, smart shadow systems, parking, and urban shelters), where the shape changes in response to distinct external stimuli. The advantages associated with the use of biomimetic model were (1) easier and faster change of shape, (2) lower need of energy for system operation, (3) lower cost for SMA training, and (4) no problem of overheating. The important thing was that the SMA was trained for a one-way effect. The problem with two-way effect was in the fact that, though it was easy and fast to heat the SMA (by electrical current), the cooling time (in the absence of external and appropriate devices) was high and depended on room temperature and the geometry of SMA.

The electrophoretic deposition (EPD) technique has a widespread application as a coating method for metallic implant, which usually releases metal ions in the body that may induce an allergic reaction on the surrounding tissues. To deal with these situations, Khalili et al. (2016) focused on the characterization of mechanical properties of hydroxyapatite-silicon-multi-walled carbon nano-tubes composite coatings—synthesized by EPD on NiTi SMAs, for biomedical applications. The cell culture results reflected on the potential of human mesenchymal stem cells to adhere and proliferate on the pure hydroxyapatite and composite coatings. The hydroxyapatite coating in the presence of both silicon and multi-walled carbon nano tubes induced more adherence of viable human mesenchymal stem cells than that of the hydroxyapatite coating with silicon alone.

NiTi biomedical SMAs have been frequently employed in different clinical applications, for instance, orthodontic therapy, prostheses, catheters, tissue anchoring and connection, cardiovascular stents, and many more. Therefore, the prevention of infections of these alloys in clinical conditions becomes key issue for orthopedic and dental surgeons. To address such issue, addition of antibacterial alloying elements can pave way for the development of novel NiTi alloys. Among various alloying elements, copper can be brought into effect as an alloying element due to the following reasons (1) displaying superior in vitro antibacterial performance, (2) preventing early biofilm formation to restrict periprosthetic infections, (3) altering the function and structure of proteins in the bacterial cell wall (leading to its consequent rupture), (4) binding and altering several bacterial enzymes (that are vital for bacterial cellular respiration and metabolism), and (5) interfering with DNA through cell division and replication. Inspired by the aforementioned facts, Li et al. (2016) had chosen copper in their study for design and development of novel ternary biomedical Ti–Ni–Cu SMAs with antibacterial properties. It was reported that Ti–Ni–Cu alloys deliver good mechanical properties and display excellent SME even after adding copper as alloying element. Ti–Ni–Cu alloys also displayed excellent antibacterial properties, possessing good cytocompatibility, which reflects the

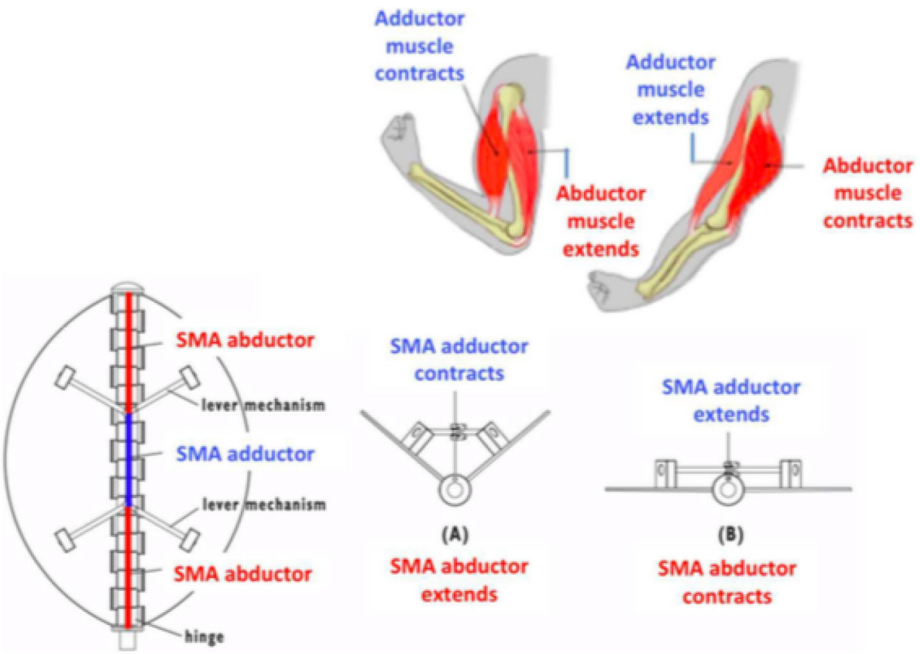


**Fig. 9** Biomechanically inspired SMA driven machine, adapted from Aversa et al. (2016)

capability of Ti–Ni–Cu alloys as future biomedical implants and devices (without inducing bacterial infections). Further, the results of the study revealed that the corrosion behavior of Ti–Ni–Cu alloys are better than the commercial biomedical Ti–50.8Ni (at%) alloys. This was mainly due to the fact that the corrosion current density steps down with addition of Cu. This results in the enhancement of the corrosion resistance of TiNi alloys and helps in preventing the release of toxic Ni ion. It is to be noted here that the toxic Ni ion release amounts of Ti–Ni–Cu alloys are less compared to that of TiNi alloy, and this is due to the addition of Cu. A schematic diagram for antibacterial mechanism of TiNiCu alloys is shown in Fig. 10.

Since superelastic alloys, like nickel-free titanium-based SMAs, possess low stiffness, high mechanical resistance with biomimetic mechanical behavior, they are often utilized for load-bearing implant applications, to overcome the risks of implantation failure. Moreover beta Ti alloys show even lower stiffness than conventional Ti alloys. Keeping these fact in mind, Sheremetyev et al. (2016) depicted functional fatigue behavior of superelastic beta Ti–22Nb–6Zr (at%) alloy for load-bearing biomedical applications. They used Ti–Nb–Zr alloy in their work, as this alloy bears capability to involve both biological compatibility and mechanical compatibility. The results obtained from fatigue testing revealed that the highly dislocated alloy (450 °C) indicated the longest fatigue life for the smallest strains (0.2%), whereas for higher strains (> 0.3%), the nanosubgrained alloy (600 °C) signified the best fatigue performance (because of the superelasticity in the deformation process). The study also reported that the blending of biocompatible alloy components, high elongation to failure, static and dynamic functional properties, and low Young's modulus made the nanosubgrained superelastic Ti–22Nb–6Zr alloy extremely acceptable for orthopedic implant applications. As a factor of risk for

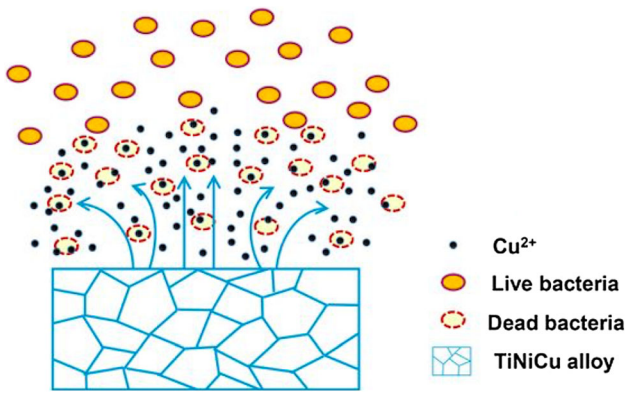


**Fig. 10** Schematic diagram for antibacterial mechanism of TiNiCu alloys, adapted from Li et al. (2016)

implant applications, the only lacuna of Ti–Ni SMAs is the availability of toxic nickel in their composition that opens the door for the development of nickel-free SMAs. When developing new load bearing biomaterials, biomechanical compatibility and biochemical compatibility as prime aspects of biocompatibility need to be effectuated. Based on these notions and with an aim to develop novel load bearing biomaterials, Prokoshkin et al. (2016) focused on the development and characterization of Ni-free SMAs, in particular, Ti–Nb-based alloys for biomedical applications. They employed smelting technology to obtain small and medium size ingots of selected compositions. For a general assessment of the mechanical, chemical, and biological aspects of compatibility of these alloys, the outcomes of their mechanical, electrochemical, and in vitro cytotoxicity testing were presented. It was concluded that Ti–Nb–Zr alloy, with nanosubgrained structure after post-deformation annealing (PDA) at 600 °C for 30 min, exhibited perfect and stable low modulus superelastic behavior, when compared to Ti–Nb–Ta alloy. This reflects on the better biomechanical compatibility of Ti–Nb–Zr alloy.

The demand for enhancement of the quality of life has led to the development of new technologies, many of which can also be seen in biomedical industries. Because of its lower young's modulus and unique SME, NiTi SMA is recently identified as the next generation orthopedic biomaterial. When wear occurs, the generation of Ni-rich debris pose some problem while using NiTi SMA. To eliminate the impact of wear, by enhancing wear resistance, surface treatment is necessary. In order to fulfill these aspects, Ng et al. (2017) dealt with the surface treatment of NiTi, by laser selective area nitriding. A two-step optimization process was followed to execute this: (1) selection of laser parameters (with an L9 Taguchi experiment) to optimize the nitride properties and (2) identification of the optimized surface coverage ratio to maximize the wear resistance. Witkowska et al. (2017) worked on enhancing the properties of NiTi SMA, wherein the NiTi SMA was oxidized in low temperature plasma with carbon coating, making it a potential applicant for cardiovascular applications. The surface treatment of NiTi alloys, by employing a hybrid process under glow discharge conditions, makes it possible to produce surface layers which enhances corrosion resistance and biocompatibility. Also, it improves the properties of NiTi in terms of its contact with blood. The study revealed that NiTi SMAs, with a carbon coating formed on top of the oxide layer, gave an upper hand for use in medicine in cardiac implants, as compared to NiTi SMAs, in their initial state. As the materials applied in load bearing implants (to offer the restoration of damaged bone tissue) need to be reliable, safe, and highly functional, Konopatsky et al. (2017) focused on enhancing the structural features and cyclic

mechanical properties of ternary Ti–Zr–Nb and quaternary Ti–Zr–Nb–Ta SMAs for biomedical applications. Specifically, they obtained Ti–18Zr–14Nb, Ti–18Zr–13Nb–1Ta, Ti–18Zr–12Nb–2Ta, and Ti–18Zr–11Nb–3Ta (at%) SMAs by vacuum arc remelting, and by subjecting them to distinct thermomechanical treatment schedules. Usually, the fatigue performance of Ti–Nb-based alloys is limited by a relatively small crystallographic resource of recovery strain (nearly 3%). This limitation can be taken care by employing Ti–Zr-based alloys. The results of the study showed that the crystallographic resource of recovery strain for all the alloys exceeds 5%, and reaches 6% for the Ti–18Zr–11Nb–3Ta alloy. Moreover, the fatigue life of the Ti–18Zr–13Nb–1Ta alloy was found to be almost twice as high as that of the Ti–18Zr–14Nb alloy. It was also reported that an increment in the tantalum content, at the cost of niobium, can enhance the functional fatigue properties of Ti–Zr–Nb–Ta alloys.

The SMAs such as NiTi and NiTi-based alloys, which display SMEs at body temperature, are usually recommended in biomedical applications. With this in mind, Kök and Ateş (2017) executed a study in order to yield NiTi and NiTi-based alloys with different chemical rates and electron concentrations, and also to analyze their distinct physical properties. The transformation temperatures of Ni45–Ti55–Cr2.5–Cu2.5, Ni48–Ti51–Mn and Ni48–Ti51–Co SMAs signified a transformation below 37.5 °C (below the body temperature), while Ni45–Ti55 and Ni48–Ti51–Sn alloys exhibited transformation over 37.5 °C. The results of the study reported Ni48–Ti51–Mn alloy as the most ideal alloy, which completes the transformation at body temperature. Sun et al. (2018) provided martensite structure and mechanical properties of Ti–Nb–Ag SMAs for biomedical applications. To be specific, they systematically studied the role of addition of Ag on martensite structure, mechanical properties, and shape memory behaviors of the solution treated Ti–Nb–Ag alloys. It was observed that the addition of Ag enhances the work hardening rate, as well as ultimate tensile strength, by varying the martensite structure. It also improves the SME because of solution hardening. Moreover with Ag addition, the reversible strain of 2% was achieved in Ti–Nb alloys (owing to the solution hardening of Ag). The results showed that Ti–16Nb–1Ag alloy has a good combination of high strength (840 Mpa) and low elastic modulus.

Characterized by exceptional corrosion resistance, good ductility, and high yielding strength, titanium-based alloys are frequently utilized for biomedical applications. For instance, human body implants such as hip joints, dental implants, and medical devices, all utilize titanium-based alloys. Taking the characteristics of these alloys into consideration, Ibrahim et al. (2018a) carried out parametric optimization of microwave sintering porous Ti–23Nb (at%) SMAs for biomedical applications. By employing microwave sintering approach, they successfully fabricated porous Ti–23Nb SMAs, and then analyzed the impact of microwave sintering parameters on the microstructure, phase composition, phase transformation temperatures, mechanical properties, and SME of these alloys. Notably, the low elastic modulus of these alloys is quite helpful in avoiding the problem of stress shielding. Consequently, microwave heating can be put into effect to sinter Ti-alloys for biomedical applications. Because of the presence of pores in bulk material, porous Ni–Ti alloys are also of perpetual interest for bioimplantation to elicit in-growth of body tissue, decrease density of the alloy, and improve fixation. In order to control grain sizes and compositions, powder metallurgy fabrication processes can be employed. Drawing on these notions, Ibrahim et al. (2018b) performed powder metallurgy fabrication of porous 51(at%)Ni–Ti SMAs for biomedical applications. Emphasis was placed to trace out the influence of temperature on the microwave sintering of Ni–Ti SMA. It was found that the sintering condition of 700 °C for 15 min produced a part with coherent surface survey that does not exhibit gross defects. When the sintering time and temperature was increased, defects on the outer surface were created, whereas reduction in the temperature to 550 °C severely affected the mechanical properties. Furthermore, a significant increase in the fracture strength and slight decrease in the fracture strain was noticed when sintering temperature was increased from 550 to 700 °C. When sintering temperature was reduced from 700 to 550 °C, the corrosion behavior of Ni–Ti SMA got severely affected. On a brief note, the idea was to choose optimum parameters to come up with Ni–Ti alloys with desired properties for biomedical applications.

Attributes like, the excellent deformability, high strength, low elastic modulus, superior corrosion resistance, and non-toxicity make metastable Ti–Zr-based SMAs highly suitable for load bearing biomedical applications. Taking advantage of these attributes, Sheremetyev et al. (2018) analyzed structural and functional properties of metastable beta Ti–18Zr–14Nb (at%) alloy for biomedical applications subjected to radial shear rolling (RSR) and thermomechanical treatment (TMT). TMT is usually considered to control the structure and functional properties of SMAs. With an objective of forming distinct structures in long-length bars (meant for bone implants fabrication), a novel combination of RSR with TMT, involving cold rolling and post-deformation annealing at distinct temperatures, was employed to Ti–18Zr–14Nb SMA. To effectuate this, a 50 mm diameter and 660 mm long Ti–18Zr–14Nb ingot was created by induction skull melting and was isostatically pressed (900 °C, 100 MPa, 2 h). When ingot was subjected to RSR at 900 °C with total

area reduction of 48%, the process resulted in the formation of dynamically polygonized substructure, which led to a combination of high ductility (35%) and superior functional fatigue resistance. Being one of the most productive non-traditional machining processes, wire electrodischarge machining (WEDM) can operate complex shapes. Hargovind et al. (2019) studied the impact of different process parameters of WEDM viz. pulse on time, pulse off time, servo voltage, wire speed and servo feed on the material removal rate and surface roughness for machining of TiNiCo SMAs (which are usually utilized as bone staple material). The study performed by them was oriented toward the advanced machining of TiNiCo SMAs for biomedical applications.

## Shape memory alloys in aerospace arena

### Gist of past reviews

Shape memory alloys have been the region of interest among aerospace researchers for the past few decades. The prime aim of aircraft designers is to maximize the synergy of the system, by enhancing its functionalities. To achieve this goal, SMAs always manifest their worth by acting as actuators and load carrying members. Barbarino et al. (2014) presented a detailed review focusing on the application of SMAs in morphing aircraft, with special attention on variable twist, camber, actuation bandwidth, and reduced power consumption. Novel configurations were developed by them in order to maximize integration and effectiveness of SMA actuators (by exploiting SME). It was pointed out that a number of developed structural configurations for morphing applications these days involve SMA wires or SMA rods. They stressed on the necessity of iterative and multi-disciplinary modeling, because of the fluid–structure interaction mingled with nonlinear thermomechanical behavior of SMAs. This review article is the most recent review article concerning applications of SMAs in the field of aerospace.

Quan and Hai (2015) discussed the utilization of shape memory alloy in aircraft hydraulic system, and the feasibility of attaining the notion of self-adapting deformable wing. They outlined the experience of using SMA in hydraulic system, and shared the difficulties and the requirements that are needed in practice. As an important aspect, they emphasized on the enhancement of the self-adapting potential of SMAs at high and low temperatures, for even more widespread use of SMAs. It was reported that the application of SMA tube in sealing connection of hydraulic system on Y12F airplane was a breakthrough, and this was also the first large-scale utilization of SMA in domestic aviation field. Further, the advantages of SMA connection are (1) SMA tube fittings is lighter (over 60%) than traditional tube fittings (2) compression performance can reach 5000 Psi and even more for special SMA tube (3) the cost of SMA tube connection is 40% cheaper than traditional tube (4) corrosion resistant feature of TiNi based SMA, and (5) the ease of installation and operation. Though it has some advantages but its processing comes with few technical difficulties, namely (1) the material production requirement is very high (2) the material preparation issue needs to be resolved (3) difficult to design and manufacture the tube joint. With the rise of SMA components used as actuators, quite a good amount of adaptable aero-structural solutions are available. But, due to the lack of industry or government-accepted standardized test methods for actuators employing SMAs, their transformation to commercialization and production level has been obstructed. To address this issue, Hartl et al. (2015) presented a brief fast track communication pertaining to an initiated collaborative and pre-competitive SMA specification and standardization effort. This could lead to the first ever regulatory agency-accepted material specification and test standards for SMAs used as actuators for commercial applications.

Since high performance actuating mechanisms are required in aerospace applications, the importance of SMAs become paramount. The SME empowers SMA to restore its pre-determined shape via thermal cycles, which makes it an ultimate choice in use as actuators. Compared to hydraulic actuators, SMA actuators are simpler, lighter, silent and need lower voltages for operation. Observing the necessity of enhancing and developing novel actuators, powered by SMA, to improve aircraft performance, Karagiannis et al. (2017) developed two actuation approaches based on SMA wires, which are quite capable of imparting efficient wing morphing. The first approach was focused on aerofoil skin morphing by involving embedded SMA wires within the composite plate, while the second one placed emphasis on morphing the internal structure of the wing by deforming the leading edge of a rib using the compliant mechanism notion. The advantageous features, such as compactness, ability to absorb loads, and transmission of large forces as well as deformations, offered by SMAs, to the designers, can lead to the simplification of many systems, provided these alloys are utilized as monolithic actuators. Influenced by this, Ameduri et al. (2016) worked on the landing gear for unmanned aerial vehicles (UAV) (that is integrated with SMA springs as actuation devices). The UAV system relied on two subsystems, viz. deployment and locking. These subsystems were actuated through SMA springs, whose retraction was ensured by other identical springs behaving in antagonistic way.

Shape memory alloys are usually employed in active (use as actuators) and passive (dissipation of vibration energy) control problems. Since their hysteretic behavior imparts energy dissipating and damping potentials, these

alloys have received increasing interest in passive control problems. Drawing on this, Sousa et al. (2018) numerically analyzed the profound influences of the pseudoelastic hysteresis of SMA springs on the aeroelastic behavior of a two degree of freedom (plunge and pitch) typical airfoil section, for six distinct sets of alloy constitutive properties. Along with the preloaded and non-preloaded SMA springs, the aeroelastic behavior for each set was compared for a range of airflow speeds in post-flutter condition. It was concluded that the aeroelastic behavior was sensitive to the set of SMA properties, and also sensitive to the preload too.

The SMA actuators attain high actuation and stress levels at the same time, and this leads to a high volumetric energy density of these alloys. Aerodynamics interplay with outer shape and airflow and, therefore, SMA FRP structures are interesting candidates for aerodynamic applications. SMA FRP technology allows the generation of complex curved shapes of laminar components. Moreover in terms of applications, where design space is premium, SMAs are preferable materials for lightweight products. Moved by these features, Hübler et al. (2016) unfolded the application capability of active fiber-reinforced polymer (FRP) structures, with integrated SMA elements, for novel aerodynamic functions. The researchers highlighted the advantages of hybrid SMA FRP structures, and their promising application concepts. The central focus of the researchers was the development of a new ideology, pertaining to an active aerodynamic airfoil, and realization of a hardware demonstrator. The advantages of SMA FRP structures with an active aerodynamic airfoil, which were demonstrated successfully, are (1) highly reduced design space requirements (thickness of lower shell increased to 4.5 mm), (2) high lightweight potential (30 mm wide structure of 42 g lifts 120 g and generates surface at the same time), (3) high-design freedom of surface deflection (generation of curved shapes), (4) enhanced aerodynamic performance (no kinks or gaps on the surface present), and (5) reduced complexity of assembly (only two electrical connections needed). The decreased complexity of actuated elements, and the decreased design-space and weight provide an upper hand for novel aerodynamic applications. For instance, multi-winglets and active trailing edge control (Fig. 11). These new functions on demand can be associated with the current flight situation of an aircraft. For the cruise and take-off/landing situations, a switch between multi-winglet and single winglet can help to optimize the drag. Further, trailing edge deflection also has a sound influence on the aerodynamic performance of aircrafts. Moreover, the on-demand activation of adaptive vortex generators (Fig. 11) can allow for the steeper and slower landing approaches (without an issue for the cruise efficiency). In addition to these advantages, the way of integrating SMA elements in

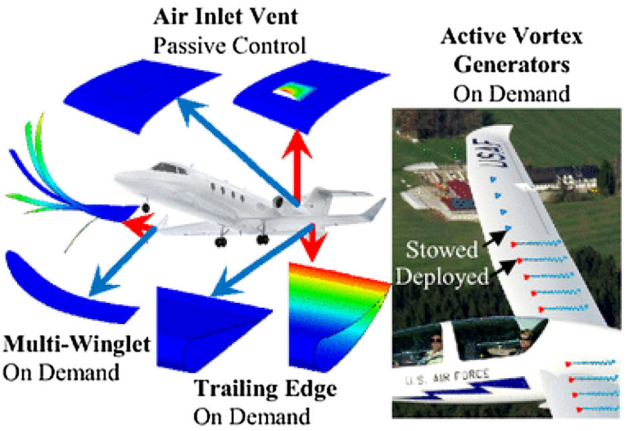


**Fig. 11** Aerodynamic application concepts for active SMA FRP structures, with permission from Springer Nature (Hübler et al. 2016)

FRP cause some difficulty in reliability, electrical connection, and manufacturing. Some drawbacks are (1) adhesive failure between SMA surface and FRP matrix, (2) large current connections waste space and influence the actuation adversely (working as a heat sink during the activation), and (3) reproducibility relating to the precise alignment during manufacture is complicated.

The phenomena of SMAs viz. superelasticity and shape memory effect are dependent on the chemical composition as well as heat treatment employed to SMA materials. Since NiTi SMAs are commercially available, they are preferred for practical applications. But there is a problem associated with NiTi SMAs. Because the transformation temperature of NiTi SMAs is lower than 100 °C, it is inconvenient to use these alloys in high temperature actuator systems that operate higher than 100 °C. Therefore, attempts have been made to shift the transformation temperature of these alloys above 100 °C without interfering with its functionality. Based on these information, DİLİBAL (2016) delineated the impact of long-term heat treatment on the thermomechanical response of NiTi SMA. This was done to shift its martensitic transformation temperature to the desired operational temperature range. The results of the study unfolded that the employed long-term heat treatment (450 °C for 100 h) increased the transformation temperature with a wide temperature hysteresis. It was also found that the operational range of the SMA was shifted to the room temperature service condition. Moreover, the presented stress–strain loading plots signified that the heat treated samples were found to be in the martensitic state at the room temperature. Dilibal concluded that the long-term heat treatment can be employed for the implementation of smart actuation and smart composite systems in aerospace industries. Leal et al. (2018) determined the optimized cruise and landing airfoil configurations, along with SMA actuator configuration needed to morph between

the two. They proposed a method for preliminary design of feasible morphing wing configurations, which are capable of imparting benefits under different flight conditions. Through their analysis, they demonstrated the possibility of fully integrated design of airfoil and distributed actuators. They also pointed out that SMA-driven reconfigurable wings are structurally possible even when stress and buckling constraints are taken into consideration.

Exarchos et al. (2018) numerically analyzed the thermomechanical responses of SMA coating, and SMA-coated metallic element, by implementing a thermomechanical SMA model, and considering Ni–Ti SMA with distinct compositions (viz. equiatomic and 50.8Ni–49.2Ti (at%) alloys). The idea behind choosing these two was that when heat treated, Ni–Ti in equiatomic composition does not form precipitates, whereas Ni-rich alloys such as 50.8Ni–49.2Ti form $Ni_4Ti_3$ precipitates. The precipitation of $Ni_4Ti_3$ particulates reduces the nickel content in the matrix, thus making it richer in titanium. This helps in strengthening 50.8Ni–49.2Ti SMA and also increasing the transformation temperature due to decrement in the nickel content. The formation of $Ni_4Ti_3$ precipitates also play vital role in the two-way SME. Bringing these two SMA compositions into effect, the authors developed a novel approach that allows to control the mechanical properties of metallic components by external stimuli, in order to enhance mechanical behavior of aluminum structures meant for aeronautical applications. The presented approach utilizes SME of novel SMA coatings, deposited on metallic structural components, with an objective to relax the stress of underlying structures, by means of simple heating at field-feasible temperatures. To perform this, a two-phase coating deposition process was executed. The SMA coating was deposited on the compressive side of a bent aluminum substrate during phase 1, while in phase 2, the SMA coating/substrate structure was unloaded to regain the original shape (as illustrated in Fig. 12). The coating resulted in improving the structural integrity, increasing the stiffness as well as rigidity of such structures, allowing them to withstand loadings safely, and protecting them from corrosion. A key factor for SMA coating to achieve SME is the appropriate heat treatment. Ni–Ti coating of equiatomic composition needs high phase transformation temperature, while the phase transformation temperature of Ni-rich coating depends on the precipitates therein. As aircraft structures, such as wing box and fuselage, are modular structures, designed using beams, the study considered a long aluminum beam with its lateral surfaces encased in SMA coating. It was reported that the SMA coatings developed on aluminum structural elements were oriented toward aeronautical applications (for instance, in the reinforcement of aircraft wing box structure and fuselage structure, to enhance their structural integrity). SMA coating ratio defined as the ratio of the SMA coating thickness to smallest dimension of the beam was considered to analyze different geometry. When SMA coating ratio of 1:400 (SMA coating thickness as 0.01 mm and smallest dimension as 4 mm, say) was used, the experienced tensile stress, once the coating was fully transformed into austenite, reaches around 780 MPa while compressive stress developed in the beam was approximately 4 MPa. A temperature (around 200 K) was required for full phase transformation. Likewise, when the SMA coating ratio was 1:50, compressive stress of approximately 30 MPa and tensile stress of around 750 MPa with temperature of approximately 200 K were figured out. Lastly, for a ratio of 1:10, the compressive stress gets increased to approximately 100 MPa and tensile stress gets decreased to around 700 MPa (with the temperature around 180 K needed for full transformation).

In order to come up with efficient and lighter aeronautical structures involving smart materials, efforts are being made to redefine morphing systems. Going with the flow, Leal and Savi (2018) provided the design of SMA actuated adaptive flap. They proposed a quasi-static fluid structure model of a flap, driven by a mechanism incorporating SMA wire and bias linear spring. The model involved thermomechanical properties for SMA wire, that was

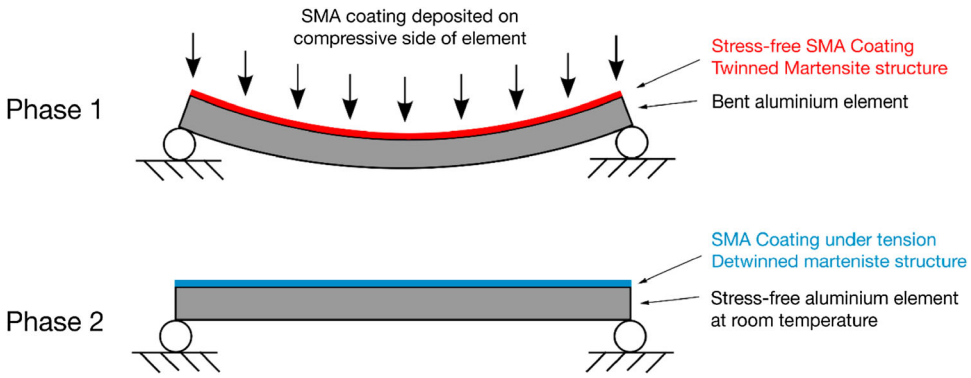


**Fig. 12** SMA coating deposition process on an aluminum substrate to obtain SME, adapted from Exarchos et al. (2018)

experimentally characterized by means of inverse problem techniques. It was concluded that, with the increment in number of degrees of freedom (design complexity), the power required to attain desired flap deflection got diminished. Shape memory alloys have high energy density and are also very power efficient. Moreover, compactness and low weight play vital role in aircraft interiors. Since SMA-based actuators are capable of diminishing weight, these alloys are ideal candidates to be considered as weight-saving materials, for lightweight construction of the interiors of aircrafts. To meet this consideration, Weirich and Kuhlenkötter (2019) analyzed the requirements in aircraft interiors with respect to possible applications of SMAs. The researchers identified various critical and noncritical requirements, for the implementation of SMA-based actuators, and suggested solutions for critical requirements, in order to provide possible applications for SMAs. They placed emphasis on the methodical development, and thorough testing of SMA-based actuator in order to come up with a reliable and precise product, so that it can also be employed in other sectors. As compactness and low weight are of keen interest in aircraft interiors, these two characteristics legitimize the partly higher costs of SMA actuators (which may cause an obstruction for using SMAs in other domains).

A cluster of critical requirements for SMA in aircraft interiors is mapped out in Fig. 13. Each requirement has been connected to the attributes and solutions that can assist in achieving the requirements. The requirement of compatibility with temperature variation primarily depends on the choice of material, as different SMAs show different range of transformation temperatures. If the actuator is assumed to operate at temperatures higher than austenite start temperature, then operation may not be reliable. This can be addressed by certain possibilities, such as changing the transformation temperature by means of tension or isolation of the casing, but these constructive measure may not work unless the choice of material is suitable. Further, the compatibility with connection energy is also critical for the utilization of SMA in aircraft interiors, due to the fact that the aircraft's energy system is limited to some voltage and current, and there might be chance of occurrence of high voltage peaks. The type of connection between energy system and actuator can be influenced by method of activation. A direct connection is not necessary if the activation is realized by means of an ambient medium. Moreover, a direct connection using heating, by electric current, may

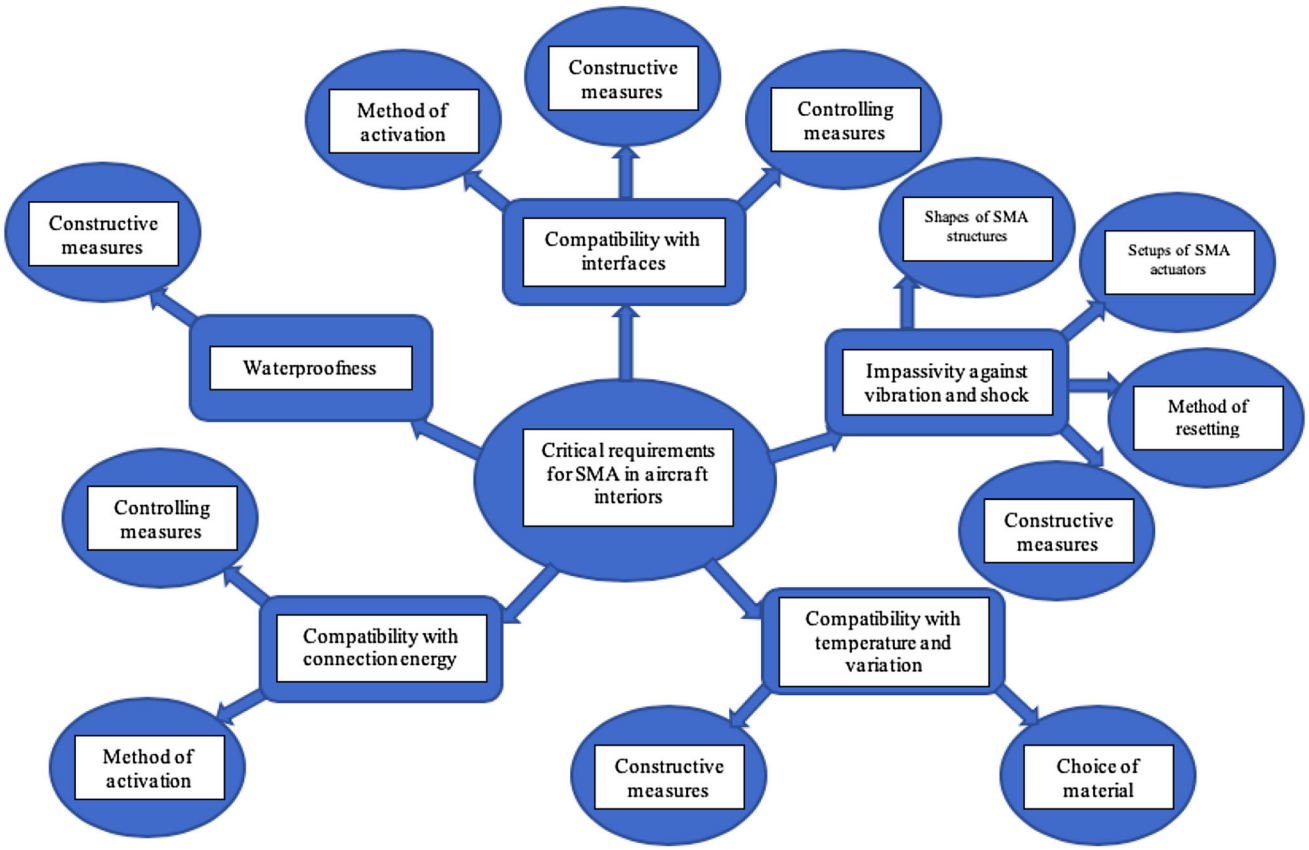


**Fig. 13** A cluster of critical requirements for SMA in aircraft interiors with SMA specific attributes, adapted from Weirich and Kuhlenkötter (2019)

be possible as controlling measure, for the protection of SMA actuator against peaks or fluctuations. In nutshell, employing controlling or constructive measures like using a hermetic sealed casing for waterproofness, and precise SMA specific actuator design for compatibility with required operation temperature, may help to address other critical requirements.

For various applications in aerospace industry that need high strength and stable actuation cycles along with transformation temperatures above 100 °C, SMAs can be employed as actuators. Aging method may be helpful in adjusting the transformation temperatures and improving the cyclic stability due to the formation of nanosized precipitates, and therefore, may be used for NiTiHf alloys. Drawing on this knowledge, to manifest the influence of aging on the stability of the actuation strain and transformation temperatures, Saygili et al. (2019) analyzed the high cycle functional fatigue life and behavior of the extruded and aged nickel rich 50.3Ni–29.7Ti–20Hf (at%) SMA. In order to check the repeatability of the shape memory properties (transformation temperature and actuation strain) of the samples, the fatigue experiments were conducted twice. It was found that the life cycle of the aged sample was 20,337 and the extruded sample lost all its shape memory behavior after 5000 cycles. It was also reported that the fatigue life of 50.3Ni–29.7Ti–20Hf alloy was improved by the aging heat treatment (550 °C for 3 h). Although, it was pointed out that the cyclic stability of the alloy in functional fatigue experiments (in terms transformation temperatures and actuation strain) was enhanced, but not fully maintained with the aging process. Hence, it was suggested that if the alloys are employed in the actuator-type applications with the requirement of high number of cycles, attention is needed.

## Shape memory alloys in offshore platform

### Theme of prior reviews

With the objective of fulfilling the demand concerning marine resources, quite a good amount of research targeting offshore platforms has been accomplished in the recent years. Multiple aspects, such as damage detection, reliability assessment, structural design, structural analysis, fatigue analysis, and structural monitoring, are featured in these offshore platform centered research. Precisely, offshore platforms can be classified into fixed-bottom platforms, and buoyant platforms—both encompassing a varied number of platforms. These platforms are often utilized to unearth, drill, yield, store, and ship ocean resources. As these platforms face stiff oceanic environment, over a long span of time, they are more prone to environmental loadings viz. waves, wind, ice, currents, earthquakes, and many more. This may lead to intense vibration of offshore platforms, resulting in structural and mechanical failures. An offshore platform under the influence of various environmental loadings is illustrated in Fig. 14.

It, therefore, becomes obligatory to ensure reliability and safety of offshore platforms, by means of equipped applicable techniques, so as to suppress and eliminate vibrations prevailing in offshore platforms. This would also avoid frequent structural maintenance and inspection. Generally, passive, active, semi-active, and hybrid methods are adopted for vibration control. To meet the aforementioned aspects and overcome challenges, shape memory alloys can be implemented into the structure of interest as passive damping, or semi-active damping elements, in order to control the configurations, structural modes, and dampen vibrations to a great extent. Focusing on the structural vibration control, Kandasamy et al. (2016) documented a review inclined toward vibration control methodologies, and the way they can be applied for marine offshore structures. Lately, a review on recent advances in vibration control of offshore platforms, incorporating passive control, and several semi-active control schemes, was provided by Zhang et al. (2017a). They also discussed various challenging issues that may pave way for the future research. Due to the high corrosion resistance property of SMAs, shape memory effect, superelasticity, and appearance of SMAs-based products (such as SMA-actuated blow out preventers, deepwater actuators, valves, underwater connectors, seals, self-torquing fasteners), SMAs have been successful in receiving attention of industrial communities. Observing the recent development and applications of SMAs in offshore platforms, Patil and Song (2017) compiled a review on shape memory materials in general; detailing their applications in the offshore oil and gas industry in particular. This review article by them is the recent available review till date on the literature exploring the potential of SMMs in offshore industries.

The coupling of pall-typed friction damper (PFD) and SMA with each other, as a brace system, can lead to the control of structural vibrations. This is due to the fact that PFD possesses high volume of energy dissipation, and SMA holds exceptional superelastic property. Reckoning on these peculiarities, Zhang et al. (2017b) analyzed vibration control of jacket (offshore) platform structures based on the SMA brace system, the ISO(isolation)-SMA brace system and the ISO-PFD-SMA brace system, which were subjected to seismic and ice-induced excitations. The considered brace systems were installed on the isolation layer of jacket platform. Specifically, PFD-SMA brace system incorporates PFD and SMA supports, wherein the connection of SMA braces and PFD steel plate are joined by bolts. A PFD-SMA brace system is exhibited in Fig. 15.

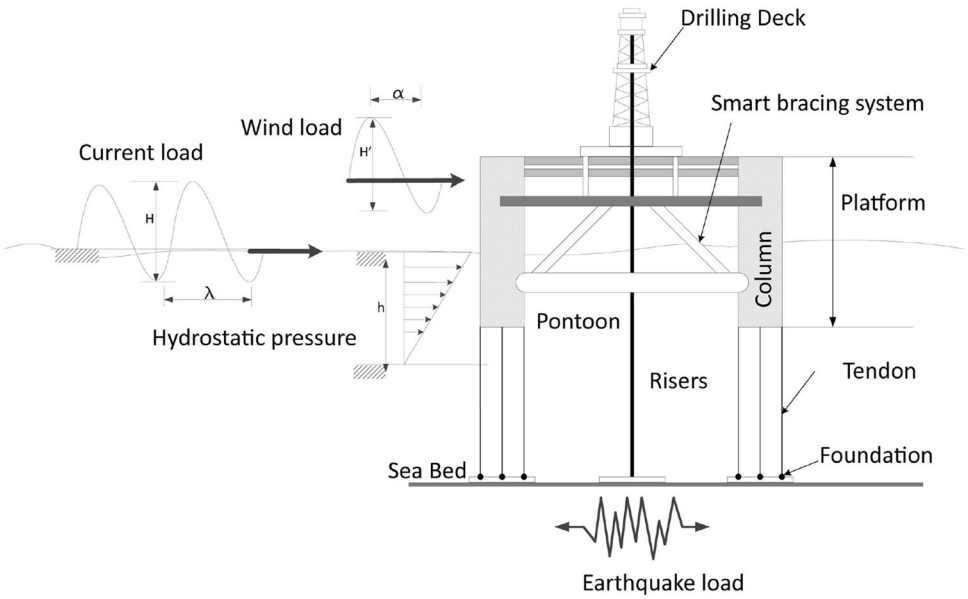


**Fig. 14** Schematic diagram of offshore platform under different environmental loads, with permission from Elsevier (Zareie et al. 2019)

The results indicated that ISO-PFD-SMA system was superior to the ISO-SMA system, due to the fact that ISO-PFD-SMA acquires 92.5% reduction on the maximum displacement of jacket under Tianjin seismic excitation (18.4% higher than ISO-SMA). Under Taft earthquake excitation, ISO-PFD-SMA system again has good control effect on the maximum displacement of jacket as the percentage of reduction was up to 80.4% (25% higher than ISO-SMA). This shows that ISO-PFD-SMA system has obvious effects on displacement suppression. However, it was found that ISO-PFD-SMA system was slightly lower on the acceleration control than ISO-SMA, but still it fulfills the security and comfort requirements. Moreover, it was also pointed out that ISO-PFD-SMA brace system possesses good self-centering capability, as the structure with ISO-PFD-SMA brace system nearly returned to the initial position after the seismic excitation. As an outcome of the study, it was remarkably traced out that the ISO-PFD-SMA brace system was quite capable in diminishing the seismic as well as ice-induced response of the offshore platform structure. This reflects the hysteretic behavior and energy dissipation potential of such system. Further, it was also concluded that only bringing SMA bracing system into play may not be helpful in achieving ideal results, as its bracing may not impart full play to their potential. This was mainly due to the fact that the overall stiffness of the structure is too large while the deformation is too small. To overcome this, it was suggested to place the damping isolation system (ISO) between the bottom of the deck and the top of the jacket structure. This may result in enhancing the energy consumption, and allow SMA bracing system to be more productive and effective.

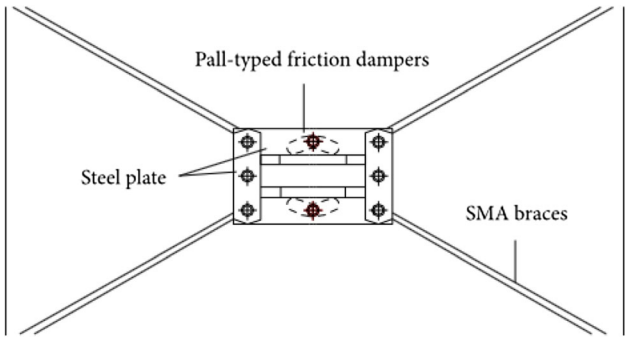


**Fig. 15** Schematic of PFD-SMA brace system, adapted from Zhang et al. (2017b)

The embedding of SMA wires in a composite laminate gives rise to shape memory alloy hybrid composite (SMAHC). With an idea to substantially decrease the operating cost, there has been keen interest among researchers concerning the improvement of hydrodynamic efficiency of marine propellers, predominantly functioning in off-design conditions, such as tugs and trawlers or a high speed attacking frigate. By inducing variable twist through heat actuation, Kapuria and Das (2018) developed a smart composite marine propeller, integrated with SMAHC actuators, in order to enhance hydrodynamic performance in off-design conditions. To complete the design aspects, they considered a full-scale marine propeller of 4.2 m diameter, which was built of graphite epoxy, with Nitinol fibers as SMA. They studied the optimal placement of SMAHC actuators for attaining maximum twist, and controlling twist, by varying temperature of SMA wires. As a conclusive statement deduced from the study, for the first time, it was possible to produce sufficient twist, that can provide the desired enhancement in the hydrodynamic performance of full-scale marine propellers in off-design

conditions. NourEldin et al. (2019) developed a hybrid damper by involving SMA bars with steel slit plate that was meant to be utilized for seismic retrofit of structures. Due to the stiffness, energy dissipation and self-centering features offered by SMA bars, the improvement in seismic performance of structures retrofitted with hybrid damper was reported through the study. The researchers also observed that the life-cycle cost of these structures was quite less, as compared to the life-cycle cost of the bare structures, and the structures having slit dampers. This was irrespective of the initial cost of hybrid damper, which was higher than the conventional slit damper. Zareie et al. (2019) designed a novel hybrid structural control element for marine structures, by taking advantages of superelasticity of SMA, and damping controllability of magneto-rheological fluid (MRF). They depicted the pronounced effect of hybrid SMA-MRF based system, on the stability of offshore structure, by adopting nonlinear time-history analysis. The results of the study remarkably signified that SMA-MRF control system profoundly enhanced the performance of marine structures under seismic loadings. It was concluded that for the structure integrated with the SMA-MRF based bracing system, the acceleration and displacement are significantly reduced as compared to the MRF-based systems only. It was also found that both the SMA and MRF systems may diminish the relative displacements under scaled ground motions, but the SMA-based systems may increase the acceleration of the marine frame structure (which is an unwanted parameter). To remove this unwanted parameter, the coupling of the MRF-based system to SMA-based system (hybrid SMA-MRF systems) can be brought into effect.

The structural functionality can get affected by undesired oscillations of jacket-type platform. With an objective to control wave-induced vibrations, Ghasemi et al. (2019) delineated the emphatic impact of optimized SMA dampers, on the improvement of dynamic behavior of jacket-type offshore structures, under the action of regular sea waves. A direct integration time history analysis was executed, and an efficient isothermal idealized constitutive model was developed by them to perform dynamic analysis, and to assess hysteretic behavior of SMA elements. It was revealed that the damper efficiency got reduced with decrement in wave intensity, and hence, it was suggested to employ active or semi-active SMA dampers, with tunable stiffness SMA elements, to control the vibrations of jacket-type platforms. They also concluded that the optimized SMA dampers can enhance the response of the structure by reducing 47.5% of deck displacement, 56.5% of deck acceleration, and 28% of base shear. The modern offshore wind turbines involve large flexible blades, which generally undergo crucial vibrations, that lead to the occurrence of fatigue in blades, and hence require frequent maintenance. To address this issue, Das et al. (2019) proposed longitudinal stiffening of blades, by incorporating tendon built of shape memory alloy, and developed a reduced order model of the combined system. By involving SMA stiffener in their model, they observed significant reduction in the displacement at the tip of the blade. The simulation results unfolded that the peak and root mean square (RMS) displacement of the blade in the out-of-plane direction got diminished by 20.58% and 30.26%, respectively, in the passive mode (stiffener without current flow). In contrast, when the current was applied, the same were obtained as 31.02% and 31.02%, respectively. Likewise, in the passive case, the peak and RMS displacement in the in-plane direction got decreased by 26.29% and 2.71%, respectively, whereas, in the active case, the same were found to be 34.65% and 9.11%. The numerical results of the study also indicated that SMA-based blade stiffening is quite helpful in reducing the mean, peak, and RMS responses, which, in turn, reflect on the enhanced reliability and fatigue life. Hence, the efficiency and advantage of SMA-based stiffener, to refine the vibrational features of the large turbine blades, were clearly demonstrated through this study.

To perform the drilling operations, and for exploitation of oil and gas resources, steel jacket platforms are usually used as offshore structures. The service life of the jacket structure and deck equipment gets decreased by wave-induced vibrations of offshore jacket platforms, thereby, incrementing the fatigue failure of the welded connections. For the purpose of vibration control and enhancement of dynamic behavior of jacket platforms, energy dissipative devices such as dampers, isolators, and dynamic absorbers can be employed. Giving shape to these ideas, Enferadi et al. (2019) analyzed wave-induced vibration control of offshore jacket platform [90 (m) high located 80 (m) deep in water] through SMA dampers, as superelasticity, high durability, and energy dissipation potential, make SMA ideal candidate for the design of vibration control devices. The proposed SMA damper used in the study is delineated in Fig. 16. The length of the damper is about 0.5 m and the outer diameter is around 0.25–0.5 m (depending on the number of SMA bars involved).

Through this study, it was reported that under the action of irregular waves, VG-SMA dampers (SMA dampers that have SMA bars with varying-geometry) avoid resonance by shifting the natural frequencies of the jacket structure away from excitation frequencies. The results of the study also reflected that CG-SMA dampers (SMA dampers that have SMA bars with constant-geometry) are capable of reducing the deck displacement/acceleration by 69%/49.8% under the action of an extreme regular wave. Further, it was pointed out that VG-SMA dampers decreased the deck displacement, deck acceleration, deck shear force, and base shear by 74.3%, 64.3%, 61.4%, and 32.1%, respectively, under the action of a 10-year return period

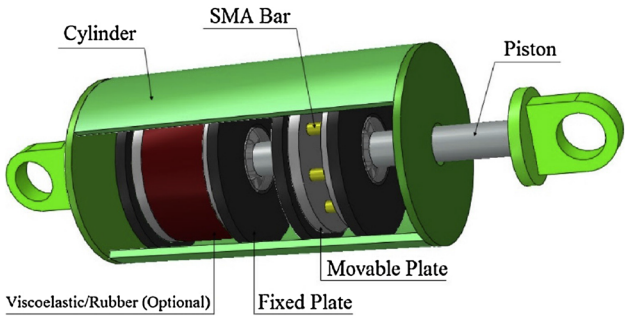


**Fig. 16** Sketch of the SMA damper, with permission from Elsevier (Enferadi et al. 2019)

irregular wave (sea state-1). Under a 100-year return period (sea state-2), the same were reduced by 65.4%, 64.7%, 62% and 22.5%, respectively. Hence, by means of this study, it was shown that VG-SMA dampers can work as semi-active devices for controlling wave-induced vibrations of the jacket platforms, although, for future studies, the authors suggested to employ VG-SMA dampers with more SMA bars geometry variations in order to suppress the vibrations in the new designed platforms.

## Conclusions

Various aspects of shape memory alloys have been discussed, studied, researched, and published for more than half a century. Although there have been regular reviews on distinct topics of interest, but in order to keep track on the current progress and development of SMAs, this documented work intends to bring together comprehensive review on modeling and diverse applications of SMAs which have been accomplished in the recent five years. To begin with, introductory notions of shape memory alloys, and their associated phenomenon have been presented concisely. Thereafter, a detailed review on the executed works concerning modeling of SMAs has been taken into account. In addition to this, recent progress on the applications of SMAs in the field of construction, biomedical, aerospace, and offshore has been reviewed exhaustively. In nutshell, the salient features of the research works carried out in considered areas of interest in the last half a decade can be outlined as follows:

1. SMAs in construction sector
    - The ductility and self-centering ability of composite with PESMA fibers is more superior as compared to steel fibers.
    - For better strengthening of concrete structures, SMA-FRPs can be brought into effect for NSM applications.
    - The use of superelastic SMA bars in NSM strengthening applications can lead to certain advantageous features such as improved bond behavior, enhanced deformation capacity and post-event functionality.
    - Cost-effective SMAs are the need of the hour as they can advocate the use of SMAs as NSM reinforcement for strengthening concrete members.
    - SMA-FRCCs hold prestressing and crack closing capabilities for enhancing structures.
    - Ni–Ti cables are required in non-bonded applications and/or in post-tensioning solutions, which may pave way for new possibilities to the structural concrete industry.
    - Fe-SMA strips can be implemented as external end-fixed reinforcements, to strengthen RC structures.
    - The fatigue life is significantly improved and the fatigue crack gets arrested by the use of prestressed Fe-SMA strips.
    - Using SMA connections in smart buildings could significantly decrease the economic loss with prominent control of undesirable residual deformations in structural fuses, because of their induced recentering behavior.
2. SMAs in biomedical domain
    - Porous Ti–Nb-based SMAs are showing their potential as promising implants for biomedical applications.
    - NiTi SMA bearing graded porosity displayed resembling mechanical performance as human long bones, and therefore, proved to be better implant candidates for the replacement of human long bone.
    - Ti–Ni–Cu alloys deliver good mechanical properties and display excellent SME, even after adding copper as alloying element. Moreover, these alloys also manifest excellent antibacterial properties, and possess good cytocompatibility. Both these properties reflect the capability of Ti–Ni–Cu alloys as future biomedical implants and devices without inducing bacterial infections.
    - Ti–Nb–Zr alloy bears capability to involve both biological compatibility and mechanical compatibility that allow this alloy to perform biomedical applications.
    - The only lacuna of Ti–Ni SMAs is the presence of toxic nickel in their composition. Because of this, there has been shift toward Ni-free SMAs, in particular, Ti–Nb-based alloys (for biomedical applications in the development of novel load bearing biomaterials).
    - NiTi SMAs with a carbon coating formed on top of the oxide layer gives an upper hand for their use in

medicine on cardiac implants as compared to NiTi SMAs in their initial state.

3. SMAs in aerospace arena
   - There is a need to increase the self-adapting ability of SMAs at high and low temperatures for their widespread utilization in aviation field.
   - For achieving novel aerodynamic functions, the advantages of hybrid SMA FRP structures is being exploited.
   - The long-term heat treatment can be employed on NiTi SMA for the implementation of smart actuation and smart composite systems in aerospace industries.
   - SMA coating induces stress relaxation to the underlying structures through SME. The coating also enhances the structural integrity, increases the stiffness as well as rigidity of the structures, thus allowing them to withstand loadings safely, and protecting them from corrosion. A key factor for SMA coating, to achieve SME, is the appropriate heat treatment.
   - SMA coating can be applied on aluminum structural elements for aeronautical applications, for instance, in the reinforcement of aircraft wing box structure and fuselage structure to enhance their structural integrity.
4. SMAs in offshore platform
   - ISO-PFD-SMA brace system is quite capable in diminishing the seismic as well as ice-induced response of offshore platform structure, which brings out the hysteretic behavior and energy dissipation potential of such system.
   - SMA-MRF control system profoundly enhances the performance of marine structures under seismic loadings.
   - Under the action of irregular waves, SMA dampers, involving SMA bars with varying-geometry, avoid resonance by shifting the natural frequencies of the offshore jacket structure away from excitation frequencies.

## Future scope of shape memory alloys

It is evident from the aforementioned facts that shape memory alloys have moved on from their initial stages, and are flourishing in the current scenario. Moreover, researchers and designers have come forward with a view to deal with concerned models, in order to envision, as well as enhance, SMA functionality to a great extent. Their better understanding in context to SMAs has boosted the success rate of these alloys in multiple applicative domains. Not only in medical applications but also in non-medical applications, they offer extraordinary performance. In order to achieve commercial success, more and more cost effective SMAs are the need of the present time. These alloys are still in their nascent state of development and application, and the vital thing is that researchers and designers should be efficient enough of finding new means to overcome the bottleneck coming in the path of the development of SMAs. Therefore, a better communication as well as interaction among concerned SMA leaders, on how to adopt, and employ distinct approaches, according to the necessity of these alloys can help them attain dizzy heights of success in near future. To wind up, smart marketing can play pivotal role in the commercialization of SMAs, in order to observe their all round development touching upon multi-dimensional region of interest.

**Acknowledgements** The authors convey their sincere thanks to the National Institute for Research and Development in Defence Shipbuilding-New Delhi (NIRDESH) and the Office of Naval Research-Global (ONRG) for supporting this work. The authors also gratefully acknowledge the University Grants Commission (UGC), New Delhi for providing Dr. D.S. Kothari Postdoctoral Fellowship to S. Kumar (through award letter No. F.4-2/2006 (BSR)/MA/17-18/0016).

## References

Abdollahzadeh M, Hoseini SH, Faroughi S (2019) Modeling of superelastic behavior of porous shape memory alloys. Int J Mech Mater Des 2019:1–13

Abidi IH, Khalid FA, Farooq MU, Hussain MA, Maqbool A (2015) Tailoring the pore morphology of porous nitinol with suitable mechanical properties for biomedical applications. Mater Lett 154:17–20

Abouali S, Shahverdi M, Ghassemieh M, Motavalli M (2019) Nonlinear simulation of reinforced concrete beams retrofitted by near-surface mounted iron-based shape memory alloys. Eng Struct 187:133–148

Alam M, Youssef M, Nehdi M (2007) Utilizing shape memory alloys to enhance the performance and safety of civil infrastructure: a review. Can J Civ Eng 34(9):1075–1086

Alipour A, Kadkhodaei M, Ghaei A (2015) Finite element simulation of shape memory alloy wires using a user material subroutine: parametric study on heating rate, conductivity, and heat convection. J Intell Mater Syst Struct 26(5):554–572

Alvandi S, Ghassemieh M (2014) Application of shape memory alloys in seismic isolation: a review. Civ Eng Infrastruct J 47(2):153–171

Ameduri S, Favaloro N, Pellone L et al (2016) A shape memory alloy application for compact unmanned aerial vehicles. Aerospace 3(2):16

Ancker C (1958) Pitch and curvature corrections for helical springs. J Appl Mech 25:466–470

Auricchio F, Petrini L (2004) A three-dimensional model describing stress-temperature induced solid phase transformations: solution algorithm and boundary value problems. Int J Numer Methods Eng 61(6):807–836

Aversa R, Tamburrino F, Petrescu RV, Petrescu FI, Artur M, Chen G, Apicella A (2016) Biomechanically inspired shape memory effect machines driven by muscle like acting NiTi alloys. Am J Appl Sci 13(11):1264–1271

Barbarino S, Flores ES, Ajaj RM, Dayyani I, Friswell MI (2014) A review on shape memory alloys with applications to morphing aircraft. Smart Mater Struct 23(6):063001

Birman V (1997) Review of mechanics of shape memory alloy structures. Appl Mech Rev 50(11):629–645

Bonilla L, Hassan MM, Noorvand H, Rupnow T, Okeil A (2017) Dual self-healing mechanisms with microcapsules and shape memory alloys in reinforced concrete. J Mater Civ Eng 30(2):04017277

Boyd JG, Lagoudas DC (1996) A thermodynamical constitutive model for shape memory materials. Part I. The monolithic shape memory alloy. Int J Plast 12(6):805–842

Cai W, Meng X, Zhao L (2005) Recent development of tini-based shape memory alloys. Curr Opin Solid State Mater Sci 9(6):296–302

Chang W-S, Araki Y (2016) Use of shape-memory alloys in construction: a critical review. Proc Inst Civ Eng Civ Eng 169(2):87–95

Chemisky Y, Duval A, Patoor E, Zineb TB (2011) Constitutive model for shape memory alloys including phase transformation, martensitic reorientation and twins accommodation. Mech Mater 43(7):361–376

Cisse C, Zaki W, Zineb TB (2016a) A review of constitutive models and modeling techniques for shape memory alloys. Int J Plast 76:244–284

Cisse C, Zaki W, Zineb TB (2016b) A review of modeling techniques for advanced effects in shape memory alloy behavior. Smart Mater Struct 25(10):103001

Cladera A, Weber B, Leinenbach C, Czaderski C, Shahverdi M, Motavalli M (2014) Iron-based shape memory alloys for civil engineering structures: an overview. Constr Build Mater 63:281–293

Cortez-Vega R, Chairez I, Luviano-Juárez A, Feliu-Batlle V (2018) A hybrid dynamic model of shape memory alloy spring actuators. Measurement 114:340–353

Dadbakhsh S, Speirs M, Van Humbeeck J, Kruth J-P (2016) Laser additive manufacturing of bulk and porous shape-memory NiTi alloys: from processes to potential biomedical applications. MRS Bull 41(10):765–774

Daghash SM, Ozbulut OE (2016) Characterization of superelastic shape memory alloy fiber-reinforced polymer composites under tensile cyclic loading. Mater Des 111:504–512

Daghash SM, Ozbulut OE (2017) Bond-slip behavior of superelastic shape memory alloys for near-surface-mounted strengthening applications. Smart Mater Struct 26(3):035020

Das S, Sajeer M, Chakraborty A (2019) Vibration control of horizontal axis offshore wind turbine blade using SMA stiffener. Smart Mater Struct 28:095025

Dehaghani PF, Ardakani SH, Bayesteh H, Mohammadi S (2017) 3D hierarchical multiscale analysis of heterogeneous sma based materials. Int J Solids Struct 118:24–40

DesRoches R, Smith B (2004) Shape memory alloys in seismic resistant design and retrofit: a critical review of their potential and limitations. J Earthq Eng 8(3):415–429

DİLİBAL (2016) The effect of long-term heat treatment on the thermomechanical behavior of NiTi shape memory alloys in defense and aerospace applications. J Def Sci/Savunma Bilmleri Dergisi 15(2):1–23

Duerig TW, Melton K, Stöckel D (2013) Engineering aspects of shape memory alloys. Butterworth-Heinemann, Oxford

Enferadi MH, Ghasemi MR, Shabakhty N (2019) Wave-induced vibration control of offshore jacket platforms through SMA dampers. Appl Ocean Res 90:101848

Eulert DD (1969) Symposium on rolamite. Technology Application Center, Institute for Social Research and Development, The University of New Mexico, and Office of Industrial Cooperation, Sandia Laboratories

Evangelista V, Marfia S, Sacco E (2009) Phenomenological 3D and 1D consistent models for shape-memory alloy materials. Comput Mech 44(3):405

Exarchos D, Dalla P, Tragazikis I, Dassios K, Zafeiropoulos N, Karabela M, De Crescenzo C, Karatza D, Musmarra D, Chianese S et al (2018) Development and characterization of high performance shape memory alloy coatings for structural aerospace applications. Materials 11(5):832

Fang C, Zhou X, Osofero AI, Shu Z, Corradi M (2016) Superelastic sma belleville washers for seismic resisting applications: experimental study and modelling strategy. Smart Mater Struct 25(10):105013

Ghafoori E, Neuenschwander M, Shahverdi M, Czaderski C, Fontana M (2019) Elevated temperature behavior of an iron-based shape memory alloy used for prestressed strengthening of civil structures. Constr Build Mater 211:437–452

Ghasemi MR, Shabakhty N, Enferadi MH (2019) Optimized SMA dampers in vibration control of jacket-type offshore structures (regular waves). Int J Coast Offshore Eng 2(4):25–35

Ghassemieh M, Rezapour M, Sadeghi V (2017) Effectiveness of the shape memory alloy reinforcement in concrete coupled shear walls. J Intell Mater Syst Struct 28(5):640–652

Gu X, Zhang W, Zaki W, Moumni Z (2017) Numerical simulation of pseudoelastic shape memory alloys using the large time increment method. Smart Mater Struct 26(4):045016

Haghdoust P, Lo Conte A, Cinquemani S, Lecis N (2018) A numerical method to model non-linear damping behaviour of martensitic shape memory alloys. Materials 11(11):2178

Hargovind S, Narendranath S, Ramesh MR (2019) Advanced machining of TiNiCo shape memory alloys for biomedical applications. Emerg Mater Res 8(1):14–21

Hartl D, Mabe J, Benafan O, Coda A, Conduit B, Padan R, Van Doren B (2015) Standardization of shape memory alloy test methods toward certification of aerospace applications. Smart Mater Struct 24(8):082001

Hashemi YM, Kadkhodaei M, Salehan M (2019) Fully coupled thermomechanical modeling of shape memory alloys under multiaxial loadings and implementation by finite element method. Continuum Mech Thermodyn 31(6):1683–1698

Hassan M, Mehrpouya M, Emamian S, Sheikholeslam M (2013) Review of self-healing effect on shape memory alloy (SMA) structures. Adv Mater Res 701:87–92

Heidari B, Kadkhodaei M, Barati M, Karimzadeh F (2016) Fabrication and modeling of shape memory alloy springs. Smart Mater Struct 25(12):125003

Heintze O et al (2004) A computationally efficient free energy model for shape memory alloys-experiments and theory. North Carolina State University, Raleigh

Huang H, Chang W-S (2018) Application of pre-stressed sma-based tuned mass damper to a timber floor system. Eng Struct 167:143–150

Hübler M, Nissle S, Gurka M, Breuer U (2016) Fiber-reinforced polymers with integrated shape memory alloy actuation: an innovative actuation method for aerodynamic applications. CEAS Aeronaut J 7(4):567–576

Ibrahim MK, Hamzah E, Nazim E, Bahador A et al (2018a) Parameter optimization of microwave sintering porous Ti–23% Nb shape memory alloys for biomedical applications. Trans Nonferrous Met Soc China 28(4):700–710

Ibrahim MK, Hamzah E, Saud SN, Nazim E (2018b) Powder metallurgy fabrication of porous 51 (at.%) Ni–Ti shape memory

alloys for biomedical applications. Shape Mem Superelast 4(2):327–336
Izadi M, Ghafoori E, Shahverdi M, Motavalli M, Maalek S (2018) Development of an iron-based shape memory alloy (Fe-SMA) strengthening system for steel plates. Eng Struct 174:433–446
Izadi M, Motavalli M, Ghafoori E (2019) Iron-based shape memory alloy (Fe-SMA) for fatigue strengthening of cracked steel bridge connections. Constr Build Mater 227:116800
Jafarzadeh S, Kadkhodaei M (2017) Finite element simulation of ferromagnetic shape memory alloys using a revised constitutive model. J Intell Mater Syst Struct 28(19):2853–2871
Jani JM, Leary M, Subic A, Gibson MA (2014) A review of shape memory alloy research, applications and opportunities. Mater Des (1980–2015) 56:1078–1113
Kandasamy R, Cui F, Townsend N, Foo CC, Guo J, Shenoi A, Xiong Y (2016) A review of vibration control methods for marine offshore structures. Ocean Eng 127:279–297
Kapoor D (2017) Nitinol for medical applications: a brief introduction to the properties and processing of nickel titanium shape memory alloys and their use in stents. Johns Matthey Technol Rev 61(1):66–76
Kapuria S, Das H (2018) Improving hydrodynamic efficiency of composite marine propellers in off-design conditions using shape memory alloy composite actuators. Ocean Eng 168:185–203
Karagiannis D, Stamatelos D, Kappatos V, Spathopoulos T (2017) An investigation of shape memory alloys as actuating elements in aerospace morphing applications. Mech Adv Mater Struct 24(8):647–657
Karamooz-Ravari M, Shahriari B (2018) A numerical model based on voronoi tessellation for the simulation of the mechanical response of porous shape memory alloys. Meccanica 53(13):3383–3397
Khalili V, Khalil-Allafi J, Sengstock C, Motemani Y, Paulsen A, Frenzel J, Eggeler G, Köller M (2016) Characterization of mechanical properties of hydroxyapatite-silicon-multi walled carbon nano tubes composite coatings synthesized by epd on NiTi alloys for biomedical application. J Mech Behav Biomed Mater 59:337–352
Khandelwal A, Buravalla V (2009) Models for shape memory alloy behavior: an overview of modeling approaches. Int J Struct Changes Solids 1(1):111–148
Kim MK, Kim DJ, Chung Y-S, Choi E (2016) Direct tensile behavior of shape-memory-alloy fiber-reinforced cement composites. Constr Build Mater 102:462–470
Kök M, Ateş G (2017) The effect of addition of various elements on properties of NiTi-based shape memory alloys for biomedical application. Eur Phys J Plus 132(4):185
Konh B, Honarvar M, Hutapea P (2015) Design optimization study of a shape memory alloy active needle for biomedical applications. Med Eng Phys 37(5):469–477
Konopatsky A, Dubinskiy S, Zhukova YS, Sheremetyev V, Brailovski V, Prokoshkin S, Filonov M (2017) Ternary Ti–Zr–Nb and quaternary Ti–Zr–Nb–Ta shape memory alloys for biomedical applications: structural features and cyclic mechanical properties. Mater Sci Eng A 702:301–311
Kramer SL et al (1996) Geotechnical earthquake engineering. Pearson Education India, New Delhi
Lagoudas DC (2008) Shape memory alloys: modeling and engineering applications. Springer, Berlin
Lagoudas D, Hartl D, Chemisky Y, Machado L, Popov P (2012) Constitutive model for the numerical analysis of phase transformation in polycrystalline shape memory alloys. Int J Plast 32:155–183
Lai M, Gao Y, Yuan B, Zhu M (2015) Effect of pore structure regulation on the properties of porous TiNbZr shape memory alloys for biomedical application. J Mater Eng Perform 24(1):136–142
Lambert TR, Gurley A, Beale D (2017) Sma actuator material model with self-sensing and sliding-mode control: experiment and multibody dynamics model. Smart Mater Struct 26(3):035004
Leal PB, Savi MA (2018) Shape memory alloy-based mechanism for aeronautical application: theory, optimization and experiment. Aerosp Sci Technol 76:155–163
Leal PB, Savi MA, Hartl DJ (2018) Aero-structural optimization of shape memory alloy-based wing morphing via a class/shape transformation approach. Proc Instit Mech Eng Part G J Aerosp Eng 232(15):2745–2759
Lecce L et al (2014) Shape memory alloy engineering: for aerospace, structural and biomedical applications. Elsevier, Berlin
Li H, Qiu K, Zhou F, Li L, Zheng Y (2016) Design and development of novel antibacterial Ti–Ni–Cu shape memory alloys for biomedical application. Sci Rep 6:37475
Liu B, Hu S, Zhang W, Zhou R, Zhang Y, Zhu Y (2017) A theoretical model for functionally graded shape memory alloy cylinders subjected to internal pressure. J Mater Res 32(7):1397–1406
Liu X, Li J, Tsang H-H, Wilson J (2018) Enhancing seismic performance of unbonded prestressed concrete bridge column using superelastic shape memory alloy. J Intell Mater Syst Struct 29(15):3082–3096
Lobo PS, Almeida J, Guerreiro L (2015) Shape memory alloys behaviour: a review. Proc Eng 114:776–783
Mas B, Biggs D, Vieito I, Cladera A, Shaw J, Martínez-Abella F (2017) Superelastic shape memory alloy cables for reinforced concrete applications. Constr Build Mater 148:307–320
Masing G (1926) Eigenspannungen und verfestigung beim messing (fundamental stresses and strengthening with brass). In: Proceedings of the 2nd international congress of applied mechanics, pp 12–17
Matsuzaki Y, Naito H (2004) Macroscopic and microscopic constitutive models of shape memory alloys based on phase interaction energy function: a review. J Intell Mater Syst Struct 15(2):141–155
Miyazaki S, Otsuka K (1989) Development of shape memory alloys. ISIJ Int 29(5):353–377
Miyazaki S, Fu YQ, Huang WM (2009) Thin film shape memory alloys: fundamentals and device applications. Cambridge University Press, Cambridge
Naresh C, Bose P, Rao C (2016) Shape memory alloys: a state of art review. IOP Conf Ser Mater Sci Eng 149(1):012054
Nematollahi M, Baghbaderani KS, Amerinatanzi A, Zamanian H, Elahinia M (2019) Application of NiTi in assistive and rehabilitation devices: a review. Bioengineering 6(2):37
Ng C, Chan C, Man H, Waugh D, Lawrence J (2017) NiTi shape memory alloy with enhanced wear performance by laser selective area nitriding for orthopaedic applications. Surf Coat Technol 309:1015–1022
NourEldin M, Naeem A, Kim J (2019) Life-cycle cost evaluation of steel structures retrofitted with steel slit damper and shape memory alloy-based hybrid damper. Adv Struct Eng 22(1):3–16
Otsuka K, Ren X (1999) Recent developments in the research of shape memory alloys. Intermetallics 7(5):511–528
Otsuka K, Wayman CM (1999) Shape memory materials. Cambridge University Press, Cambridge
Ozbulut O, Hurlebaus S, Desroches R (2011) Seismic response control using shape memory alloys: a review. J Intell Mater Syst Struct 22(14):1531–1549
Paiva A, Savi MA (2006) An overview of constitutive models for shape memory alloys. Math Probl Eng 2006:56876
Patil D, Song G (2017) A review of shape memory material's applications in the offshore oil and gas industry. Smart Mater Struct 26(9):093002

Peng H, Chen J, Wang Y, Wen Y (2018) Key factors achieving large recovery strains in polycrystalline Fe–Mn–Si-based shape memory alloys: a review. Adv Eng Mater 20(3):1700741

Pequegnat A, Michael A, Wang J, Lian K, Zhou Y, Khan M (2015) Surface characterizations of laser modified biomedical grade NiTi shape memory alloys. Mater Sci Eng C 50:367–378

Petrini L, Migliavacca F (2011) Biomedical applications of shape memory alloys. J Metall 2011:15

Pittaccio S, Garavaglia L, Ceriotti C, Passaretti F (2015) Applications of shape memory alloys for neurology and neuromuscular rehabilitation. J Funct Biomater 6(2):328–344

Prokoshkin S, Brailovski V, Dubinskiy S, Zhukova Y, Sheremetyev V, Konopatsky A, Inaekyan K (2016) Manufacturing, structure control, and functional testing of Ti–Nb-based SMA for medical application. Shape Mem Superelast 2(2):130–144

Qian H, Li H, Song G, Chen H, Ren W, Zhang S (2010) Seismic vibration control of civil structures using shape memory alloys: a review. In: Earth and space 2010: engineering, science, construction, and operations in challenging environments, pp 3377–3395

Qiao L, Rimoli JJ, Chen Y, Schuh CA, Radovitzky R (2011) Nonlocal superelastic model of size-dependent hardening and dissipation in single crystal Cu–Al–Ni shape memory alloys. Phys Rev Lett 106(8):085504

Quan D, Hai X (2015) Shape memory alloy in various aviation field. Proc Eng 99:1241–1246

Rad ZR, Ghobadi MS, Yakhchalian M (2019) Probabilistic seismic collapse and residual drift assessment of smart buildings equipped with shape memory alloy connections. Eng Struct 197:109375

Rao A, Srinivasa AR, Reddy JN (2015) Design of shape memory alloy (SMA) actuators, vol 3. Springer, Berlin

Rius JM, Cladera A, Ribas C, Mas B (2019) Shear strengthening of reinforced concrete beams using shape memory alloys. Constr Build Mater 200:420–435

Rizzello G, Mandolino MA, Schmidt M, Naso D, Seelecke S (2018) An accurate dynamic model for polycrystalline shape memory alloy wire actuators and sensors. Smart Mater Struct 28:025020

Rojob H, El-Hacha R (2017) Self-prestressing using iron-based shape memory alloy for flexural strengthening of reinforced concrete beams. ACI Struct J 114(2):523

Santos FAd, Nunes J (2018) Toward an adaptive vibration absorber using shape-memory alloys, for civil engineering applications. J Intell Mater Syst Struct 29(5):729–740

Saygili HH, Tugrul HO, Kockar B (2019) Effect of aging heat treatment on the high cycle fatigue life of Ni 50.3 Ti 29.7 Hf 20 high-temperature shape memory alloy. Shape Mem Superelast 5(1):32–41

Scalet G, Boatti E, Ferraro M, Mercuri V, Hartl DJ, Auricchio F (2017) Explicit finite element implementation of a shape memory alloy constitutive model and associated analyses. In: Proceedings of XIV international conference on computational plasticity-COMPLAS

Sepe V, Marfia S, Sacco E (2013) A nonuniform tfa homogenization technique based on piecewise interpolation functions of the inelastic field. Int J Solids Struct 50(5):725–742

Sepe V, Auricchio F, Marfia S, Sacco E (2016) Homogenization techniques for the analysis of porous sma. Comput Mech 57(5):755–772

Shahverdi M, Czaderski C, Motavalli M (2016) Iron-based shape memory alloys for prestressed near-surface mounted strengthening of reinforced concrete beams. Constr Build Mater 112:28–38

Shahverdi M, Michels J, Czaderski C, Motavalli M (2018) Iron-based shape memory alloy strips for strengthening rc members: material behavior and characterization. Constr Build Mater 173:586–599

Shajil N, Srinivasan S, Santhanam M (2016) An experimental study on self-centering and ductility of pseudo-elastic shape memory alloy (PESMA) fiber reinforced beam and beam-column joint specimens. Mater Struct 49(3):783–793

Sheremetyev V, Brailovski V, Prokoshkin S, Inaekyan K, Dubinskiy S (2016) Functional fatigue behavior of superelastic beta Ti–22Nb–6Zr (at%) alloy for load-bearing biomedical applications. Mater Sci Eng C 58:935–944

Sheremetyev V, Kudryashova A, Dubinskiy S, Galkin S, Prokoshkin S, Brailovski V (2018) Structure and functional properties of metastable beta Ti–18Zr–14Nb (at%) alloy for biomedical applications subjected to radial shear rolling and thermomechanical treatment. J Alloy Compd 737:678–683

Shirani M, Kadkhodaei M (2014) A geometrical approach to determine reorientation start and continuation conditions in ferromagnetic shape memory alloys considering the effects of loading history. Smart Mater Struct 23(12):125008

Shirani M, Kadkhodaei M (2015) A modified constitutive model with an enhanced phase diagram for ferromagnetic shape memory alloys. J Intell Mater Syst Struct 26(1):56–68

Song G, Ma N, Li H-N (2006) Applications of shape memory alloys in civil structures. Eng Struct 28(9):1266–1274

Song G, Patil D, Kocurek C, Bartos J (2010) Applications of shape memory alloys in offshore oil and gas industry: a review. In: Earth and space 2010: engineering, science, construction, and operations in challenging environments, pp 1551–1567

Sousa VCd, De Marqui Junior C, Elahinia MH (2018) Effect of constitutive model parameters on the aeroelastic behavior of an airfoil with shape memory alloy springs. J Vib Control 24(6):1065–1085

Souza AC, Mamiya EN, Zouain N (1998) Three-dimensional model for solids undergoing stress-induced phase transformations. Eur J Mech A/Solids 17(5):789–806

Spaggiari A, Dragoni E (2014) Analytical and numerical modeling of shape memory alloy negator springs for constant-force, long-stroke actuators. J Intell Mater Syst Struct 25(9):1139–1148

Spaggiari A, Dragoni E (2017) Analytical modelling of rolamite mechanism made of shape-memory alloy for constant force actuators. J Intell Mater Syst Struct 28(16):2208–2221

Spaggiari A, Dragoni E, Tuissi A (2015) Experimental characterization and modelling validation of shape memory alloy negator springs. J Intell Mater Syst Struct 26(6):619–630

Sun B, Meng X, Gao Z, Cai W (2018) Martensite structure and mechanical property of Ti–Nb–Ag shape memory alloys for biomedical applications. Vacuum 156:181–186

Urbano MF, Cadelli A, Sczerzenie F, Luccarelli P, Beretta S, Coda A (2015) Inclusions size-based fatigue life prediction model of NiTi alloy for biomedical applications. Shape Mem Superelast 1(2):240–251

Van Humbeeck J (2001) Shape memory alloys: a material and a technology. Adv Eng Mater 3(11):837–850

Van Humbeeck J, Chandrasekaran M, Delaey L (1991) Shape memory alloys: materials in action. Endeavour 15(4):148–154

Van Viet N, Zaki W, Umer R (2018) Analytical model for a superelastic timoshenko shape memory alloy beam subjected to a loading–unloading cycle. J Intell Mater Syst Struct 29(20):3902–3922

Viet N, Zaki W, Umer R (2018) Analytical model of functionally graded material/shape memory alloy composite cantilever beam under bending. Compos Struct 203:764–776

Wang Q, Wu N (2011) A review on structural enhancement and repair using piezoelectric materials and shape memory alloys. Smart Mater Struct 21(1):013001

Wang J, Moumni Z, Zhang W (2017) A thermomechanically coupled finite-strain constitutive model for cyclic pseudoelasticity of polycrystalline shape memory alloys. Int J Plast 97:194–221

Wang J, Zhang W, Zhu J, Xu Y, Gu X, Moumni Z (2019a) Finite element simulation of thermomechanical training on functional stability of shape memory alloy wave spring actuator. J Intell Mater Syst Struct 30(8):1239–1251

Wang B, Zhu S, Zhao J, Jiang H (2019b) Earthquake resilient RC walls using shape memory alloy bars and replaceable energy dissipating devices. Smart Mater Struct 28(6):065021

Weirich A, Kuhlenkötter B (2019) Applicability of shape memory alloys in aircraft interiors. Actuators 8(3):61

Wilson JC, Wesolowsky MJ (2005) Shape memory alloys for seismic response modification: a state-of-the-art review. Earthq Spectra 21(2):569–601

Witkowska J, Sowińska A, Czarnowska E, Płociński T, Borowski T, Wierzchoń T (2017) Niti shape-memory alloy oxidized in low-temperature plasma with carbon coating: characteristic and a potential for cardiovascular applications. Appl Surf Sci 421:89–96

Wu S, Lin H (2000) Recent development of tini-based shape memory alloys in taiwan. Mater Chem Phys 64(2):81–92

Xu R, Bouby C, Zahrouni H, Zineb TB, Hu H, Potier-Ferry M (2018) 3D modeling of shape memory alloy fiber reinforced composites by multiscale finite element method. Compos Struct 200:408–419

Xu L, Baxevanis T, Lagoudas DC (2019) A three-dimensional constitutive model for the martensitic transformation in polycrystalline shape memory alloys under large deformation. Smart Mater Struct 28(7):074004

Yamauchi K, Ohkata I, Tsuchiya K, Miyazaki S (2011) Shape memory and superelastic alloys: applications and technologies. Elsevier, Berlin

Yoneyama T, Miyazaki S (2008) Shape memory alloys for biomedical applications. Elsevier, Berlin

Yu C, Kang G, Kan Q (2018) An equivalent local constitutive model for grain size dependent deformation of NiTi polycrystalline shape memory alloys. Int J Mech Sci 138:34–41

Yuan B, Zhu M, Chung C (2018) Biomedical porous shape memory alloys for hard-tissue replacement materials. Materials 11(9):1716

Zainal M, Sahlan S, Ali M (2015) Micromachined shape-memory-alloy microactuators and their application in biomedical devices. Micromachines 6(7):879–901

Zaki W, Moumni Z (2007) A three-dimensional model of the thermomechanical behavior of shape memory alloys. J Mech Phys Solids 55(11):2455–2490

Zaki W, Viet N (2018) Analytical model of shape memory alloy helical springs. In: ASME 2018 conference on smart materials, adaptive structures and intelligent systems. American Society of Mechanical Engineers Digital Collection

Zareie S, Alam MS, Seethaler RJ, Zabihollah A (2019) Effect of shape memory alloy-magnetorheological fluid-based structural control system on the marine structure using nonlinear time-history analysis. Appl Ocean Res 91:101836

Zhang B-L, Han Q-L, Zhang X-M (2017a) Recent advances in vibration control of offshore platforms. Nonlinear Dyn 89(2):755–771

Zhang J, Ma Z, Liu F, Zhang C, Sharafi P, Rashidi M (2017b) Seismic performance and ice-induced vibration control of offshore platform structures based on the ISO-PFD-SMA brace system. Adv Mater Sci Eng 2017:15

Zhao Y, Taya M, Kang Y, Kawasaki A (2005) Compression behavior of porous NiTi shape memory alloy. Acta Mater 53(2):337–343

Zhou D, Gao Y, Lai M, Li H, Yuan B, Zhu M (2015) Fabrication of NiTi shape memory alloys with graded porosity to imitate human long-bone structure. J Bionic Eng 12(4):575–582